GEOLOGIC MAP OF A PORTION OF THE SALT RIVER CANYON AREA AND THE GEOCHEMISTRY OF THE TOMATO JUICE URANIUM MINE, GILA COUNTY, ARIZONA

BY

JEFFREY ALLAN BRUNEAU

SUBMITTED IN PARTIAL FULFILLMENT
OF THE REQUIREMENTS FOR THE DEGREE OF
MASTER OF SCIENCE IN GEOLOGY

NEW MEXICO INSTITUTE OF MINING AND TECHNOLOGY
SOCORRO, NEW MEXICO
MAY 1981

This text is dedicated to Doug Martin, geologist, whose dedication to the science of exploration geology has inspired uncompromising spirit and dedication in all who have worked with him.

ABSTRACT

A twenty square mile area adjacent to the Salt River in Gila County, Arizona was mapped on a scale of one inch equals two thousand feet. The younger Precambrian Lower Dripping Spring Quartzite, Upper Dripping Spring Quartzite, Mescal Limestone, Troy Quartzite and diabase units are exposed in the mapped area.

The Upper Dripping Spring Quartzite with its uranium deposits is the main concern of this paper. Because of the strong structural control of the vein deposits, an airphoto structural map was compiled. Four prominent directions of lineaments were recognized (N15E, N50E, S60-65E, and S5-15E). This pattern is typical of the younger Precambrian sediments of the region which characteristically have two roughly orthogonal fracture sets of distinctly different ages.

A gamma-ray spectrometer survey was done to analyze for radiometric uranium, potassium and thorium. The survey indicated a general decrease in K and Th upwards in the Upper Dripping Spring Quartzite. Uranium concentrations are generally constant except for the base of the Black facies unit which shows anomalous concentrations of uranium.

The Tomato Juice Mine, a vein-type deposit, was geochemically sampled. It was recognized that a varied suite of elements is concentrated in the vein (Pb, Zn, Mo, As, F and U, and to a lesser extent, Cu, Ni, Co, Ag, Sb, Be and P). Samples from the host rock, a diabase sill, and a contact iron skarn deposit within the map area show trace metal suites similar to that noted in the Tomato Juice vein. It is uncertain what bearing this has on the genesis or subsequent history of the Tomato Juice vein.

It is concluded that the Tomato Juice vein was formed during a regional uplift that occurred after the deposition of the Mescal Limestone and before the deposition of the Troy Quartzite and prior to the intrusion of the extensive diabase units. The source of the metals in the Tomato Juice vein is thought to originate in the host rock itself, from the volcano-pyroclastic sedimentary component of the Black facies detritus.

TABLE OF CONTENTS

TABLE OF CONTENTS (CONT.)

FIGURES

TABLES

PLATES

INTRODUCTION

The Salt River Canyon area is located in eastern Gila County, Arizona along U.S. Highway 60 and Arizona State Highway 77, approximately 40 miles northeast of Globe, Arizona. The area mapped is located in the Globe district of the Tonto National Forest, adjacent and to the west of the San Carlos Apache Indian Reservation. Access to the area is through a county maintained road leading to the Regal Canyon and Phillips Canyon asbestos mines. It leaves the main highway at the Seneca Lake Resort, located 4.8 miles south of the Salt River Canyon bridge on U.S. Highway 60. Steeper portions of the area are accessible only by foot, but numerous dirt roads reach most of the area. The roads are generally built in a weathered-diabase, clay-rich soil which is very slick and muddy during rainy seasons, commonly in July-August and December-January.

The central portion of the mapped area is capped by diabase and Troy Quartzite forming a hilly plateau-like area. Vehicle travel across this rolling terrain is very good.

Cutting into the central area are deeply incised canyons. Vehicle travel on roads in some of the canyons is rugged and a four-wheel drive vehicle is required.

The steep drainage-incised perimeter of the area, from 3000 to 4000 feet in elevation, has a transitional type vegetation between the Sonoran Desert type and the higher elevation evergreen forests. The lower elevations have prickly pear, cholla and an occasional saguaro cactus with cats claw, various species of agave, several desert flowers and desert grasses.

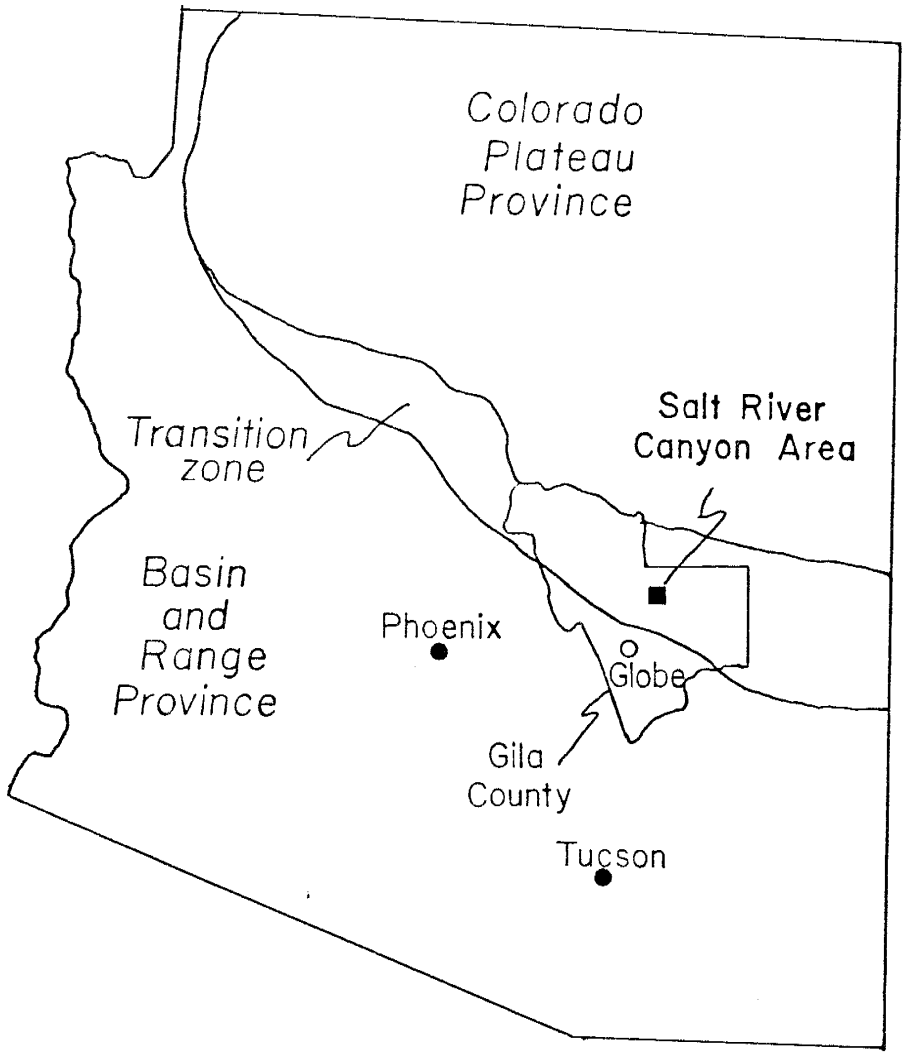

figure 1: Location map of the Salt River Canyon Area
modified after Cuffney 1977

scale
0 50 100 miles
Scale: approx. 1 inch = 80 miles

At higher elevations, 4000 to 5000 feet, scrub oaks and dwarf evergreens become prominant.

The plateau-like uplands are from 4800 to 5500 feet in elevation and are covered by a very diverse mixture of evergreens, cacti and desert grasses.

Geologic Setting

The thesis area is in the transitional zone between the Colorado Plateau and the Basin and Range geologic provinces. Most of the exposed younger Precambrian rocks in Gila County, Arizona exhibit a Colorado Plateau type structure, i.e. generally flat-lying sedimentary rocks.

Younger Precambrian rocks consist of the Apache Group sediments, the Troy Quartzite and diabasic rocks. The lower portion of the Apache Group, i.e. the Scanlan Conglomerate and the Pioneer Formation, are not exposed locally. The rock units exposed in the thesis area are the Dripping Spring Quartzite, the Mescal Limestone and the Troy Quartzite intruded by sill-like diabase units.

Previous Investigations

Regionally, there is extensive geologic literature on the younger Precambrian geology of Gila County, Arizona. The preponderance of literature is the studies of Granger and Raup, 1959 and 1964. Little of this literature, however, deals directly with the thesis area, but the regional homogeneous nature of the Dripping Spring Quartzite allows regional data to be useful locally.

Granger and Raup (1964) in their stratigraphy of the Dripping Spring Quartzite, studied the Snakebit Canyon section in the southwest portion of the study area and measured a stratigraphic section there. There have been several short descriptive works generated on the Tomato Juice uranium mine, located in the northwest part of the study area in the lower portion of Regal Canyon. Schwartz (1978) includes a map of the Tomato Juice mine in his compilation of the uranium occurrences in Gila County, Arizona. Granger and Raup (1959 and 1969) also briefly describe the Tomato Juice mine in their studies on uranium deposits in the Dripping Spring Quartzite.

General Geology

The Precambrian in Arizona has been informally grouped into two major divisions: The older Precambrian, composed of meta-sediments, meta-pyroclastics and meta-volcanics intruded by granitic stocks, is the first division. The younger Precambrian, the second division, is composed of weakly metamorphosed sedimentary rocks and lies unconformably upon the older Precambrian.

The older Precambrian metamorphic rocks of Arizona have been designated as the Vishnu schist, exposed in the Grand Canyon and the Pinal schist near Globe. These groups of meta-sediments vary lithologically and in degree of metamorphism, but represent the same general sedimentary-volcanic sequence.

Regionally, all of these units have been folded and faulted and later intruded by granitic rocks.

Livingston (1969) has dated older Precambrian meta-sediments in the White Ledges area (studied by Cuffney, 1976) located just to the south of the mapped area at 1510 m.y.

Granger and Raup (1964) tabulate the age dates from various authors giving a range of dates for older Precambrian granitic plutons from 1210 to 1660 m.y. The age of the younger Precambrian (the Apache Group, the Troy Quartzite and diabase) is bracketed by the age of the older Precambrian granitic rocks and younger Precambrian diabases that intrude these sediments.

The diabases have been dated by Neuerburg and Granger (1960) at 1100 m.y. (Pb/Pb, galena and uraninite), by Silver (after Granger and Raup, 1964) at 1075 $\pm$ 60 m.y. (Pb/Pb, zircons), and by Damon, et. al. (1961) at 1140 $\pm$ 40 m.y. (K-Ar, biotite).

The younger Precambrian, thus, is younger than approximately 1200 m.y. and older than about 1100 m.y.

Acknowledgements

I sincerely appreciate the diverse group of persons responsible for bringing this project to its fruition. Funding for this study was provided by the Phillips Uranium Corporation. I would like to make special mention of Lewis Teal of the Phillips Uranium Corporation for his many hours spent in the field and for the hours of discussions concerning this thesis and to Bill Via who spent his time and talents to guide me in the writing of this thesis.

I would also like to acknowledge the guidance, assistance and the time offered me by my thesis committee, Dr. Douglas G. Brookins, Dr. Jacques Renault, and Dr. Clay T. Smith, Chairman.

ROCK UNITS

Introduction - The Younger Precambrian

The Apache Group sediments consist of the Pioneer Shale, the Dripping Spring Quartzite and the Mescal Limestone with its associated basalt flows (see Fig. 2).

The Pioneer Shale is composed of a basal conglomerate member called the Scanlan Conglomerate. The Scanlan Conglomerate was classified as a distinct formation until it was recognized that the Pioneer and Scanlan represent a single continuous depositional unit.

The Dripping Spring Quartzite is divided into two formations: The Lower Dripping Spring Quartzite (LDSQ) with its basal Barnes Conglomerate and the Upper Dripping Spring Quartzite (UDSQ). The LDSQ is composed of massive arkosic sandstone and the UDSQ is a thin-bedded, arkosic siltstone.

The overlying Mescal Limestone is divided into three members: The lower member is thin-bedded and consists of cherty dolomite or limestone. The middle or algal member is composed of massive stromatolitic limestones and dolomites. The upper or argillite member, which is best developed in the Sierra Ancha Mountains, is composed of arkosic argillites. Above the middle algal member and above the upper argillite member there appear regional horizons of basalt flows. Locally, the basalt flows and the argillite member have been removed by erosion.

The Troy Quartzite, overlying the Apache Group, has been regionally divided into three members: The lower member is only present in northwest Gila County and is composed of well-sorted arkose. The

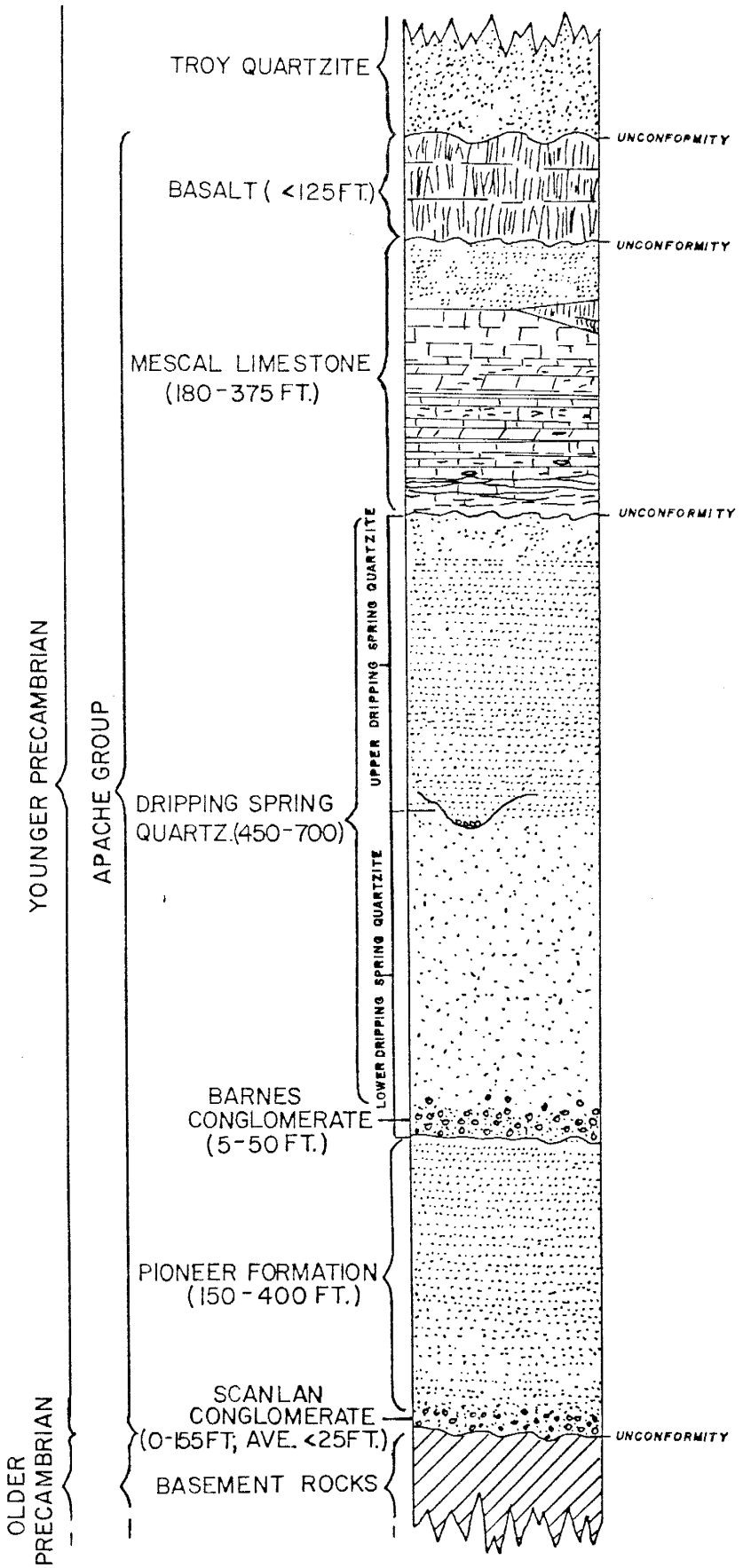

Figure 2 : Generalized younger Precambrian stratigraphic section, modified after Granger and Raup, 1959

middle or Chediski Sandstone Member is made up of pebbly, feldspathic sandstones. The upper member is composed of clean, well-sorted quartzites.

Sometime after the Troy deposition and lithification, diabase sills were intruded throughout the younger Precambrian sequence. These diabase sills often comprise up to 50 percent of the stratigraphic thickness of the younger Precambrian. They caused asbestos and iron skarn deposits to be formed in the Mescal Limestone but apparently have not otherwise greatly metamorphosed the sediments.

The Apache Group sediments were deposited in a broad, shallow basin, suggested by Granger and Raup (1964) to represent a large, marine embayment, perhaps contemporaneous but separate from the Grand Canyon series to the north.

The Pioneer was laid down on a peneplain developed upon the older Precambrian granites and metamorphic rocks. The Scanlan Conglomerate represents a marine transgression and the Pioneer a long period of sea shallowing. The Pioneer contains a large percentage of waterlaid, felsic volcanic tuffs. The base of the Dripping Spring Quartzite, the Barnes Conglomerate, represents another transgression. The Dripping Spring Quartzite represents a similar event as that producing the Pioneer. The Dripping Spring Quartzite does not contain large quantities of tuffs; it is composed of arkosic to quartzitic sediments. The Gray unit of the Dripping Spring Quartzite, however, may contain small quantities of felsic pyroclastic material. These two formations may represent a reoccurrence of a similar tectonic event. The Mescal Limestone was deposited unconformably upon the Dripping Spring Quartzite under shallow marine to intertidal environments.

The Troy Quartzite seems to represent a change in the tectonic pattern of the region. It is deposited on an unconformity at the top of the Mescal, upon which karst features are locally developed (Shride, 1967) as well as extensive erosion of the upper member. Regionally, the Apache Group sediments do not vary greatly, even in areas marginal to the basin of deposition. The Troy, however, changes in character as it approaches its basin margins (Shride, 1967). This suggests that the long, constant, stable environment of deposition of the Apache Group ended and less constant environments prevailed during Troy times. After the deposition of the lower member of the Troy Quartzite, a long period of erosion occurred and the middle and upper Troy were deposited upon this unconformity.

DRIPPING SPRING QUARTZITE

Introduction

The Dripping Spring Quartzite (DSQ) is extensively exposed throughout Gila County, Arizona and ranges in thickness from about 450 to 708 feet (Granger and Raup, 1964). It was deposited in a shallow inland sea, the shape of which is generally outlined by Granger and Raup (1964) with isopach maps and sedimentary structural data. The thickest sections appear in an east-west trend across Gila County and the DSQ thins to the northwest and southeast.

The DSQ consists of a basal conglomerate, the Barnes Conglomerate, the Lower Dripping Spring Quartzite (LDSQ), and the Upper Dripping Spring Quartzite (UDSQ). The Barnes Conglomerate member was originally classified as a formation by Ransome in 1903, but most recently it

has been given member status by Granger and Raup in 1964. The LDSQ has been previously termed the arkose member by early authors and the middle member by Granger and Raup. Presently, the LDSQ includes the Barnes Conglomerate and the middle member.

The LDSQ and UDSQ roughly equally divide the DSQ (see Fig. 3). They differ dramatically in bedding features, grain size and color. The LDSQ is composed of thick to massive bedded, pinkish arkoses, feldspathic sandstones and orthoquartzites. The UDSQ consists of thin to slabby-bedded, gray to buff arkosic to feldspathic siltstones and argillite to feldspathic sandstones. They also differ in their nature of outcrop. The UDSQ tends to be less resistant than the LDSQ forming a readily distinguishable discontinuity in weathering type at their contact.

LOWER DRIPPING SPRING QUARTZITE

Barnes Conglomerate

The Barnes Conglomerate forms the base of the LDSQ. It is generally 5 to 20 feet thick, but can be as much as 50 feet or more (Granger and Raup, 1964). No regional pattern in thickness exists.

The pebbles and cobbles of the Barnes are derived from older Precambrain terrain. No erosional windows through the underlying Pioneer Formation are known which suggests a distant source for the Barnes detritus. The Barnes is composed of pebbles and cobbles consisting of quartzites, pegmatitic quartz and small amounts of jasper, feldspar and granitic stones. The matrix is composed of from 40 to 85 percent quartz with the remainder being feldspar and alteration products of feldspar (Granger and Raup, 1964).

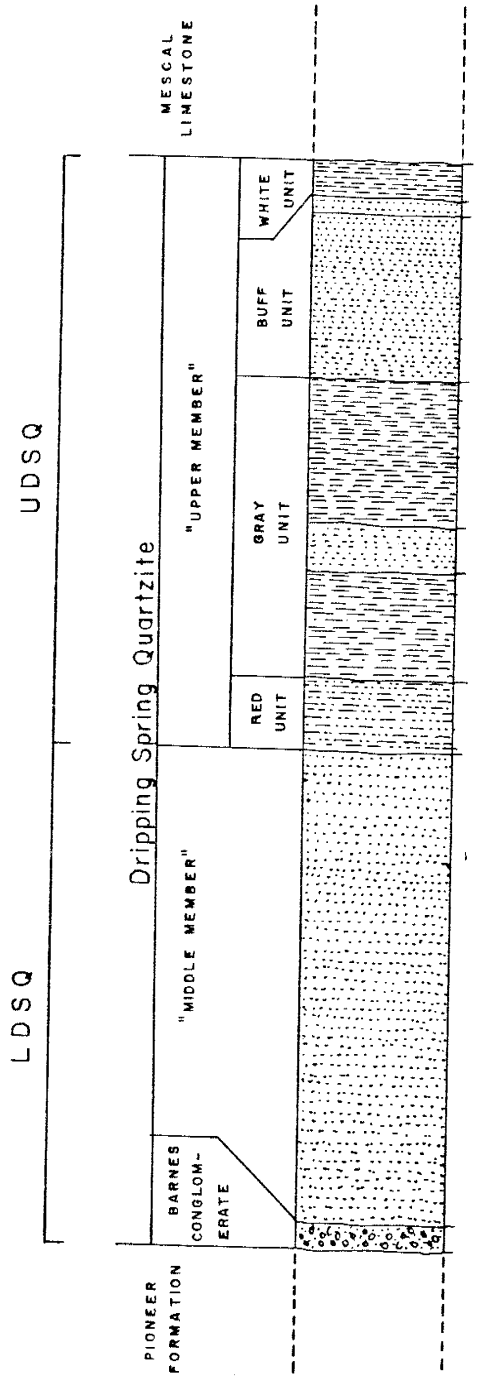

EROSIONAL DISCONFORMITY

White unit: 0-124 feet; siltstone, thinly and evenly stratified, light to dark gray.

White quartzite marker: 0-14 feet; orthoquartzite and sandstone; quartzose to feldspathic; fine to coarse grained; ledge forming.

Buff unit: 41-168 feet; sandstone, feldspathic to arkosic, light-colored, very fine grained to fine-grained, stylolites, abundantly cross-stratified.

Black facies: 13-120 feet; sandstone, arkosic, dark-gray, flaggy, thinly and irregularly stratified; crumpled shrinkage cracks.

Gray sandstone and barren quartzite: 5-6 feet; sandstone and orthoquartzite; feldspathic, commonly a fine-grained sandstone ledge capped by medium- to coarse-grained orthoquartzite.

Gray facies: 16-127 feet; siltstone, arenaceous, arkosic, light-gray, flaggy, thinly stratified; pseudochannels.

Red unit: 0-80 feet; siltstone and sandstone, micaceous, reddish.

Middle member: 0-369 feet; sandstone and orthoquartzite; conglomeratic and arkosic near base, quartzose near top; moderate red near base, grayish pink near top; very fine-grained to coarse-grained; slabby to massive, cross-stratified.

Barnes conglomerate member: 0-50 feet; conglomerate and sandstone; arkosic matrix; well rounded stones.

EROSIONAL DISCONFORMITY

Figure 3. Generalized columnar section of the Dripping Spring Quartzite, Gila County, Arizona; modified after Granger and Raup, 1964.

The Barnes Conglomerate does not outcrop within the study area. It is reported to outcrop to the west of the mapped area where it overlies a large diabase sill that has intruded at approximately the base of the LDSQ in this area (verbal communication, Showalter, 1980).

Lower Dripping Spring Quartzite Above the Barnes

Granger and Raup's middle member lies conformably upon the Barnes Conglomerate and this contact is often gradational. The middle member ranges in thickness from 140 feet to nearly 370 feet as reported by Granger and Raup (1964) in their Coolidge Dam and Roosevelt Dam stratigraphic sections, respectively. It is chiefly composed of medium-grained, firmly cemented feldspathic, orthoquartzitic sandstones. There is a general trend for individual beds to become increasingly coarser grained and less feldspathic upward through the section.

The Lower Dripping Spring Quartzite (LDSQ) consists of tabular beds with cross stratification. Often the units are so well indurated that the cross stratification is hidden or obscured. The stratification is also more obvious in the lower more feldspathic units than in the upper orthoquartzitic beds.

Shride (1967) describes the bedding as being generally greater than 4 feet thick but having a range from 4 to 6 inches to 12 to 20 feet thick.

Gastil (1953) attempted to subdivide the middle member into what he termed alpha, beta and gamma members. Locally, the LDSQ can be divided into smaller units but presently it is difficult or impossible to correlate these divisions with distant sections. At present, no stratigraphic subdivisions are made in the LDSQ.

Irregularly throughout the area mapped the upper 50 feet of the LDSQ outcrops as a tabular unit overlying a large diabase sill or complex of sills that forms the present substrate for the Salt River. Just to the west of the mapped region a complete section of the LDSQ is seen.

UPPER DRIPPING SPRING QUARTZITE

General Statement

Granger and Raup (1964) divided the Upper Dripping Spring Quartzite (UDSQ) into four units (Red unit, Gray unit, Buff unit and White unit). The Red unit forms the base of the UDSQ and ranges in thickness from 0 to 83 feet. The Red unit is absent in the northwest part of Gila County and becomes thicker to the south and southeast (Granger and Raup, 1964). The Red unit consists of interbeds of red to maroon hematitic, micaceous, arenaceous siltstones and fine-grained sandstones.

The Gray unit overlies the Red unit with a conformable, often gradational contact. The Gray unit has been subdivided by Granger and Raup (1964) into the Gray facies, the Gray sandstone, the Barren quartzite and the Black facies. The Gray unit ranges in thickness from 56 to 264 feet, thinning toward the margins of the Apache embayment. The Gray unit is composed of thin-bedded to slabby, carbonaceous, arkosic siltstones and argillites in the Gray and Black facies to feldspathic orthoquartzites in the Gray sandstone and the Barren quartzite.

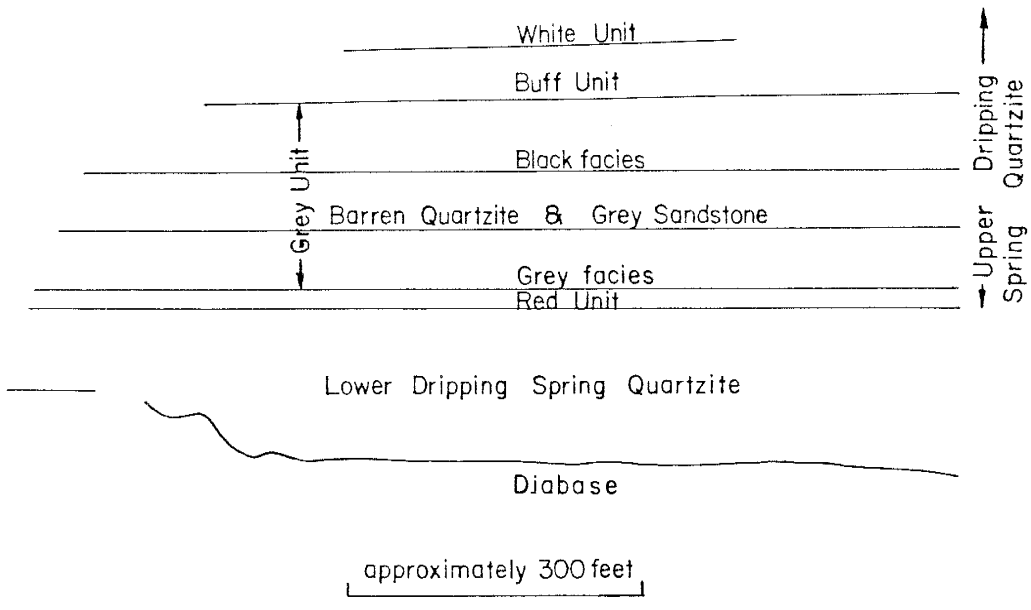
White Unit
Buff Unit
Grey Unit
Black facies
Barren Quartzite & Grey Sandstone
Grey facies
Red Unit
Upper Dripping Spring Quartzite
Lower Dripping Spring Quartzite
Diabase
approximately 300 feet

Figure 4. Exposures of the Upper Dripping Spring Quartzite along the Salt River Canyon, located in the W½, NW¼, Section 17, T. 5 N., R. 17 E.

The Buff unit overlies the Gray unit transitionally. The zone of transition varies from a typical 5 to 10 feet, as noted by the author in Regal Canyon, to approximately 40 to 50 feet as observed in Snakebit Canyon. The transition zone is characterized by interbeds of black to gray arkosic siltstones typical of the Black facies and the buff, coarser grained, quartzitic sandstones characteristic of the Buff unit. The Buff unit generally ranges from 41 to 180 feet in thickness and is capped by a thin (0 to 14 feet), white quartzite marker bed.

The White unit overlying the Buff is generally very thin. Granger and Raup (1964) report a range of thicknesses from 0 to 124 feet. The maximum thickness is observed in the Sierra Ancha Mountains in north-central Gila County, Arizona. The White unit was observed to be 8 feet thick and 42 feet thick in Snakebit Canyon and Regal Canyon, respectively.

Black Facies

Throughout the thesis study area the Black facies has a 55-foot thick basal portion with a 5 to 50-foot lithology transitional with the overlying Buff unit.

The occurrence of uranium deposits in the Upper Dripping Spring Quartzite (UDSQ) has been noted by various authors (i.e. Granger and Raup, 1959 and 1969 and Williams, 1957). The vast majority of the known uranium deposits are vein type with the upper and lower extent of the vein contained totally within the Black facies. The few exceptions are the stratiform deposits of the Suckerite Mine, Sky Prospect, Lucky Boy Mine and a deposit in the Workman Creek area recently discovered by Wyoming Minerals Corporation.

Granger and Raup (1964) describe the Black facies as follows: "The Black facies is predominantly a medium, dark-gray, laminated siltstone with a few interstratified lenses of coarser grained sandstones, particularly near the base. Stratification ranges from very thinly laminated to thin-bedded, but is mostly laminated. Sandstone and orthoquartzite lenses near the base of the facies may be cross-laminated and some of the siltstone shows wispy cross-lamination."

"The splitting property of the Black facies varies from outcrop to outcrop. In drill cores the splitting property is commonly massive or blocky. Weathering, however, has the effect of destroying the cementation along certain planes of stratification that are rich in pyrite, carbon, mica or clays, and thus the splitting property at the surface ranges from papery to blocky (see Fig. 5). Pyrite-filled stylolites are particularly susceptible to surficial oxidation, which commonly results in a flaggy or platy outcrop."

"The fresh rock ranges from very light gray to dark gray. In some places almost the entire facies is medium to dark gray, in other, light gray laminae alternate with dark gray laminae. Very thin to thin beds are commonly graded from very fine-grained sandstone at the base to silt at the top. In these the silt may be dark gray and the sandstone light gray to very light gray. The gray is largely due to the presence of very finely divided carbon and, to a lesser extent, pyrite."

Granger and Raup (1964) report (on an analysis from a small number of samples) that the Black facies siltstones consist of 60 to 90 percent potassium feldspar. The feldspars are monoclinic and un-

Figure 5. Typical bedding of the Black facies as seen in Snakebit Canyon near the base of the Black facies.

twinned with a composition of Or_{95} $(Ab + An)_5$. This possibly indicates authigenic growth of feldspars at low temperatures or crystallization in a Na free environment. Granger and Raup suggest that because igneous, pyroclastic and metamorphic feldspars have higher Na content, the feldspar is authigenic. The remainder of the rock is predominantly quartz, minor clays, plagioclase, muscovite and zircon with varying amounts of carbon and pyrite.

SEDIMENTARY STRUCTURES OF THE BLACK FACIES

The sedimentary structures are crucial in understanding the paleoenvironment of the Black facies. Recently, unpublished reports by Park, Kessler and Teal (1981) have demonstrated the similarity of some of these sedimentary structures to those produced by modern stromatolitic blue-green algal mats, growing on sandy substrates. The sedimentary structures of the Black facies consist of laminations, occasional ripple marks, abundant dessication cracks, fucoid marks, stylolites and what Granger and Raup (1964) term "pseudochannels."

Laminations are generally parallel but low angle cross-lamination is common. Laminations are usually 1/16-inch or finer. Often laminated beds have unlaminated or apparently unlaminated zones 1/4 to 1-inch or more thick composed of very fine feldspathic sandstones. An individual laminae is generally graded, fining upwards and capped by a black, very thin carbonaceous layer. Carbonaceous material also appears as spotty or pervasive disseminations.

Dessication cracks are abundant in the Dripping Spring Quartzite (DSQ). They generally form random patterns as opposed to typical polygonal patterns. The cracks are usually filled with very fine sandstone detritus, commonly with laminae curling upwards at the edges in zones of abundant carbon.

Fucuoid marks are occasionally seen on bedding surfaces. They consist of randomly oriented, shallow, elongate impressions about 1/4 by 1/2 inches often only a few hundredths of an inch deep. These marks are believed to be generated by the marine algae fucus or impressions left by seaweed.

Stylolites are extremely prevalent throughout the Upper Dripping Spring Quartzite (UDSQ) (Fig. 6 and 7). They consist of a carbon surface exhibiting "irregular and interlocking or mutual interpenetrations of the two sides, the columns, pits, teeth-like projections on one side fitting into their counterparts on the other. As usually seen in cross section, it resembles somewhat a suture..." (Glossary of Geology, 1977). Stylolites are believed to form during diagenesis by differential movement during sediment compaction. Stylolites in the Black facies are often seen separating very fine sandstone and siltstone laminae without apparently otherwise affecting continuous laminations. A fine wedge of sandstone can penetrate a laminated zone of silt, penetrating laminae but not deforming the laminations on either side of this embayment.

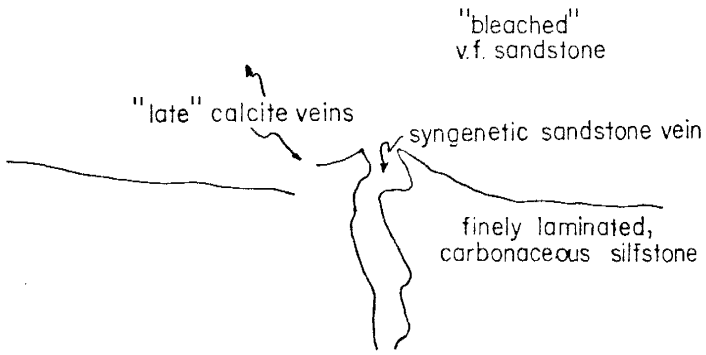
"bleached"
v.f. sandstone
"late" calcite veins
syngenetic sandstone vein
finely laminated,
carbonaceous silfstone

Figure 6. Photograph of polished section (Sample 9917) showing a typical sandstone-filled fracture/mudcrack and curling of carbonaceous layers associated with it. Curling is possibly due to the differential compaction of the sediment, but may in part be due to dessication of the mud prior to the deposition of the overlying sandstone and fracture fill.

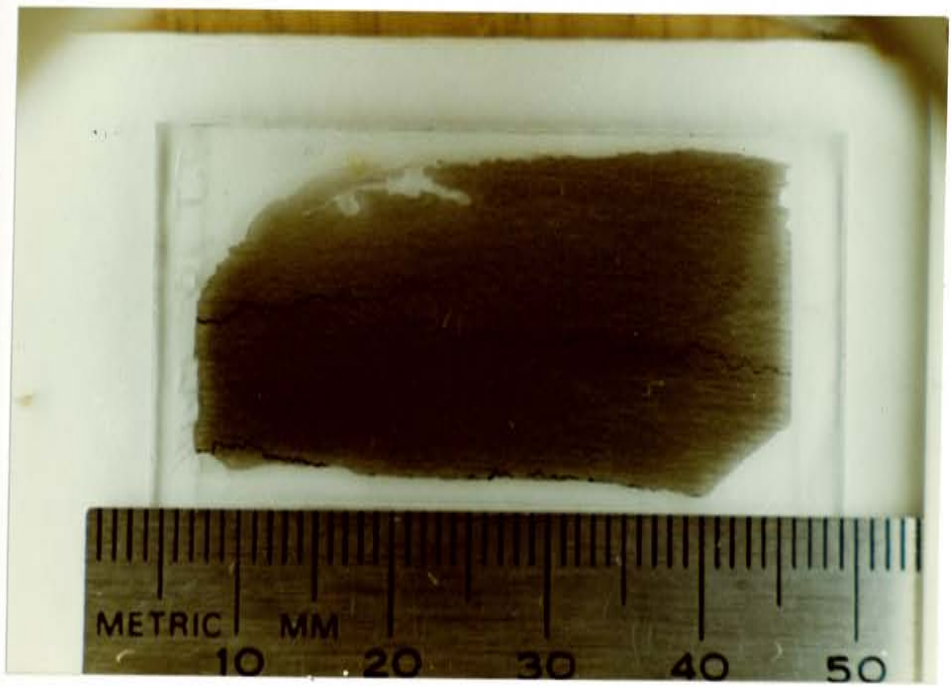

Figure 7. Photograph of thin section (Sample TJ19) showing stylolites typical of the Black facies of the Upper Dripping Spring Quartzite.

Cigar-shaped channels, generally of U-shaped cross section, were described by Granger and Raup (1964) as pseudochannels. They exist on a scale of centimeters to almost a meter in depth. They characteristically have a steep walled outline, often with internal lamination and cross-lamination not related to the host rock and are coarser grained than the surrounding rocks. Especially in small scale pseudochannels, carbonaceous laminations of the host rock will curve upwards near the top of the channel and downwards near the base of the channel until they line the bottom of the channel conformably. A model based on the growth of algal mats in a tidal flat channel is a possible explanation for pseudochannels (see Fig. 8).

Ripple marks are rare in the Black facies but where found, they are due to current oscillations. Large scale oscillations in bedding have wavelengths of 4 to 18 inches across. Granger and Raup (1964) believe these to be a form of ripple marks. The author has noted, and Kessler (1981) reports a north 5 to 25 degrees east orientation to these undulations.

MESCAL LIMESTONE

The Mescal Limestone is divided into three members (Shride, 1967): The lower thin-bedded member; the middle massive, algal member; and the upper argillite member. Subaerial vesicular basalt flows separate the middle and upper members and also cap the Mescal, but within the area mapped no basalt was noted. The upper member is only seen in the southeastern portion of the map area (Sections 12 and 13, T. 4½ N., R. 17 E.) as a thin, perhaps 5 feet or less, unit cropping out as an

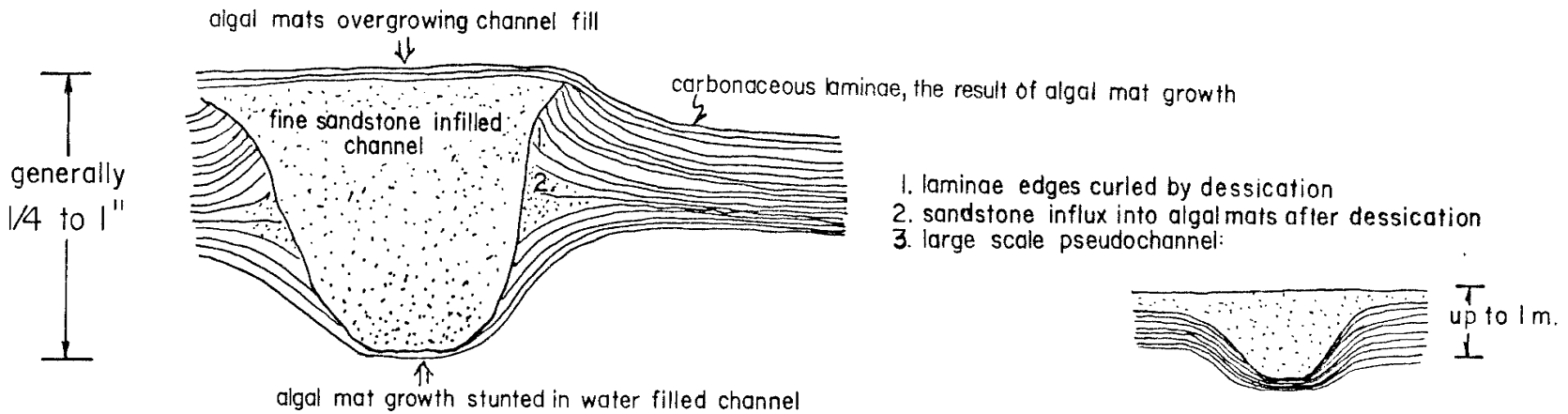

Figure 8. A model for the formation of "pseudochannels" by algal stromatolite mats. Pseudochannels of up to a meter in depth are common (3). They differ from the above diagram only in that they generally do not show upcurled laminae at the bank of the channel and the laminae tend to parallel the edge of the channel fill. The channels are formed by run-off during periods of low tide in broad tidal flats where algal mats grow in abundance.

accumulation of an argillitic to shaly regolith. Also, the upper argillite member is seen in drill holes occurring as a thin (0 to 15 feet) isolated horizon surrounded by diabase in Sections 29 and 30, T. 5 N., R. 17 E.).

At the base of the Mescal and below what is typically called the lower thin-bedded member there is a local discontinuous sandstone bed (0 to 15 feet thick) formed from the erosion of the top of the Upper Dripping Spring Quartzite (UDSQ) before limestone deposition. The lower thin-bedded member (regionally 150 to 270 feet thick) consists of thin- to thick-bedded, light gray dolomites with occasional thin chert layers and lenses. Within the map area, chert is rare and the dolomite has been metamorphosed to calcitic limestone. Two lithologies dominate the lower member in the study area: 1) Fine to medium-grained, recrystallized limestones that form resistant beds and 2) Nonresistant beds of very fine limestone that weather to earthy , chalk-like beds. On fresh outcrops these chalk-like beds do not appear significantly different from the coarser grained limestone interbeds.

The middle member (regionally 50 to 100 feet thick) is characterized by massive-bedded, light gray dolomites composed of algal stromatolite mats. The stromatolites are characterized by a wave-like cross section (see Fig. 9). In the middle of the algal member the stromatolites are hemispherical and grade above and below into the characteristic wave-like form. The internal structures of the stromatolite mats have been destroyed by recrystallization and only the external form remains.

Figure 9. Photograph of typical stromatolite bedding in the Algal member of the Mescal Limestone.

The upper member is poorly exposed in the map area and consists of gray to dark gray argillites and siltstones. Regionally, the upper member is up to 100 feet thick and is best developed in the Sierra Ancha (S.A.) Mountains. It is characterized by a base of a few inches up to 10 feet of a chert breccia or conglomerate (S.A. area only). The majority of the upper member is composed of yellowish-brown, flaggy to massive-bedded, laminated, siliceous argillites. Interbeds of gray to black shaly argillites form a subordinate lithology.

Basalt flows regionally cap the Mescal Limestone and separate the middle and upper members in the central portion of the Mescal depositional basin located in the Sierra Ancha Mountains. The basalt flows are typically vesicular and/or amygduloidal. In outcrop the color of the basalt ranges from grayish-red to reddish-black or brown and occasionally pale brown to dark yellowish-brown. The basalts have abundant disseminated hematite which imparts a blackish-red color to fresh basalt (Shride, 1967).

TROY QUARTZITE

The Troy Quartzite has three members, only two of which are regional in extent (Shride, 1967): The Arkose member, the Chediski Sandstone member and the Quartzite member. The members are not distinguished on the geologic map. The Arkose member is limited to the area surrounding the highest portions of the Sierra Ancha Mountains in the McFadden Peak 15-minute quadrangle (Shride, 1967). At or near the base of the Arkose member are conglomeratic sandstones (5 to 20 feet thick) composed of well-rounded, older Precambrian quartzite and rhyolite pebbles and cobbles in an arkosic sandstone matrix

similar to the overlying arkose beds. Above the conglomerate beds are thick to massive, tabular bedded, fine- to medium-grained, pale red to grayish-red or light to pale brown, well-sorted arkosic sandstones. The Arkose member has obvious large-scale cross stratification which readily distinguishes it from the similar appearing Lower Dripping Spring Quartzite. The Arkose member does not occur within the mapped area.

In the center of Section 20, T. 5 N., R. 17 E. on a northerly trending ridge, there is a conglomerate composed of siltstone pebbles in a clean, well-rounded quartzite matrix. This is apparently a local conglomerate at the base of the Chediski Sandstone member which is common in areas not underlain by the Arkose member. Primarily, the Chediski is composed of white sericitic sandstones. The Chediski comprises about half of the maximum outcrop thickness of the Troy within the map area, approximately 200 to 250 feet.

The overlying Quartzite member is readily distinguished from the Chediski member by the red hematitic staining of the Quartzite member which is an otherwise clean quartzite unit.

DIABASE

Precambrian (approximately 1100 m.y.) diabases coextensively intrude the younger Precambrian sediments. The diabase predominantly occurs as horizontal sills and to a lesser extent discordant bodies. In southern portions of Gila County the diabase is concordant but the complex block-faulting (Basin and Range structure) conceals this to a large extent.

The diabase (generally an olivine diabase to albite diabase) is chiefly composed of labradorite, clinopyroxene and olivine or albite and either pyroxene or amphibole. "All variations between olivine diabase and albite diabase have been seen in one sill" (Shride, 1967). The diabase is a fine- to coarse-grained holocrystalline rock with an ophitic or subophitic texture (Shride, 1967). Within the diabase, feldspathic differentiates are occasionally seen. They are diabase pegmattites, aplites and granophyric rock bodies.

The diabase intrudes older Precambrian rocks, Apache Group sediments and the Troy Quartzite. The preponderance of sills, however, intrudes the Upper Dripping Spring Quartzite and the Mescal Limestone. The sills extend over large distances and can often be traced for several miles.

Within the map area and throughout the Salt River Canyon area, sills are concentrated at the contact between the Lower and Upper Dripping Spring Quartzite and between the Mescal Limestone and Troy Quartzite. They also extensively intrude the Mescal Limestone.

The large thicknesses of sills in the Salt River Canyon area appear, in part, to be the result of multiple injections. The thin, tabular islands of Mescal in diabase are slivers which mark the contact of successive intrusions.

There are several areas on the map that exhibit radically discordant diabase intrusions ($NW\frac{1}{4}$, $NW\frac{1}{4}$, Sec. 34, SE Sec. 21 into $SW\frac{1}{4}$, Sec. 22, T. 5 N., R. 17 E., Sec. 13 and Sec. 23, T. 5 N., R. 16 E.). The discordant bodies in Sections 21, 22 and 34 are fed by subvertical dikes and expand into poorly formed laccolithic bodies.

In Section 13, two sills become discordant as they are traced towards the west. One sill (200 feet thick) cross-cuts bedding rising approximately 300 feet vertically through the Upper Dripping Spring Quartzite and then parallels horizontal bedding once more on the west side of the discordancy. The other sill is lower in the section and also cross-cuts bedding farther to the west than the first, gradually cross-cutting the section. In the SW¼, Section 23, a 300-foot sill transgresses up the section. In the center of Section 23 discordant diabase of uncertain geometry follows what appears to be a north-northwest trending, steeply-dipping fault.

On a small scale throughout the Salt River area the diabase sills often have step-like discordant contacts with sedimentary rocks. In contact with the Mescal these step discordancies are generally at very sharp right angles and are on the scale of one to several feet. Step discordancies in the Dripping Spring Quartzite are less angular than those in the Mescal and are generally subvertical and often rise up to 50 feet (see Fig. 4).

STRUCTURE

Introduction

A principal portion of the younger Precambrian in Gila County lies in the transitional physiographic province between the Colorado Plateau and the Basin and Range Provinces. In the transition zone the younger Precambrian rocks exhibit a Colorado Plateau structural type. In the south part of Gila County the younger Precambrian is extensively block-faulted where it is part of the Basin and Range province.

The Colorado Plateau is typified by generally flat-lying, undeformed sediments. Kelly and Clinton (1960) outline the major structural elements of the Plateau province as consisting of: 1) basins, 2) uplifts, 3) monoclinal flextures, 4) domes of igneous intrusions, 5) platforms, slopes and broad saddles, and 6) fold and fault belts. Not all of these structural elements are seen in the younger Precambrian. The younger Precambrian structure is characterized by generally flat-lying undeformed sediments with monoclinal flextures and normal faulting. Also, a regional orthogonal fracture pattern is observed in the younger Precambrian as is often the case in Colorado Plateau sediments.

Older Precambrian Structure

Wilson (1939) and Anderson (1951) discuss the regional structural character of the older Precambrian. The older Precambrian consists of folded metamorphic rocks, extensively intruded by granitic batholiths. The folds have northwest, north or northeast axes.

Low angle thrust faults dipping to the southeast are prevalent in the Mazatzal Mountains area. High angle normal faulting is common throughout the older Precambrian with trends paralleling the fold axes. Perpendicular to the northwest fold axes, vertical tear faults with lateral displacements of a few hundred feet cut the pre-Apache rocks.

Younger Precambrian Structure

Fractures

Williams (1957) compiled extensive data on fracture (joint) patterns in the Dripping Spring Quartzite (DSQ). The results indicate two ages of regional fracturing. They consist of two mutually bisecting orthogonal patterns. The early pattern trends north 5 to 25 degrees east and north 65 to 85 degrees west. An airphoto structural analysis done during this study confirms these joint systems (see Plate 3, Airphoto structure map). These early fractures contain the vein uranium deposits characteristic of the DSQ. The later fracture system is another orthogonal set that bisects the earlier system (e.g. north 20 to 40 degrees west and north 50 to 70 degrees east).

Models for the Genesis of Orthogonal Fractures

Large regions of undeformed sediments (for example the Colorado Plateau) often exhibit orthogonal fracture systems. The genesis of these fracture systems is variously modeled. John Gibbons (1981) believes that these patterns could be caused by the interaction of load pressure and pore fluids. Contrary to this approach, N. J. Price (1966 and 1974) proposes a model utilizing stresses generated during regional uplift due to the removal of load stress and the horizontal dilation of sediments. Other models for the genesis of orthogonal patterns call for the propagation of basement rock stresses or basement rock fracture systems, and earth tides to generate stresses and subsequent fracturing.

Gibbons' model (1981) uses a simple presentation of the Mohr stress-strain diagram. The maximum and minimum stresses in a rock are defined as sigma 1 and sigma 3, respectively. In the Gibbon's model (1981) they are due to load pressures only, i.e. no regional compressive or tensional stresses exist other than those produced by lithostatic load. When pore fluid is added, either externally or derived by expulsion of fluid during compaction, the fluid reduces the internal stresses on the rock. In doing so the Mohr stress circle moves to the left. If enough pore fluid is present, the circle will move (sigma 1 and 3 will be decreased) until the Mohr stress circle intersects the fracture envelope. Upon doing so, rock failure will occur.

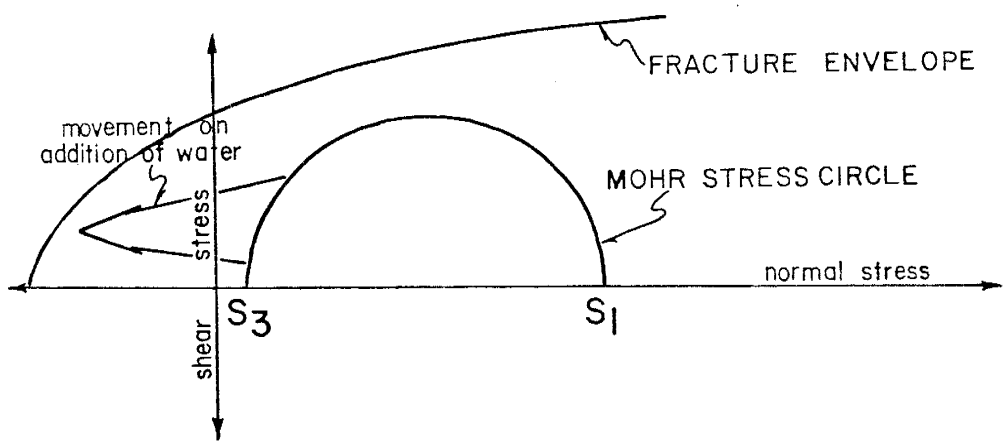

Figure 10, Mohr stress diagram explaining the fracturing of rock by load stress and water.

Gibbon's (1981) states that an isotropic (homogeneous) material failing in this way should produce polygonal fracture patterns similar to those seen in dessicated mud. Since, however, sedimentary rocks are not homogeneous, orthogonal patterns might be produced.

Price's model of fracturing during uplift uses the known physical properties of rocks. In Price's (1966) publication he states that rocks, at least in the upper levels of the crust, approximate an ideal Bingham substance. A Bingham substance is one that exhibits linear viscous deformation above a yield point (a specific stress level); and below that point is assumed to be rigid. The model implies that on burial the rock is at a pressure and temperature above which it deforms viscously. That is, the rock is viscously (plastically) compressed. After uplift and erosion, the pressure and temperature fall below this yield point and the rock becomes brittle. The mathematics of the dilation (horizontal expansion) due to uplift are simple (see Fig. 11).

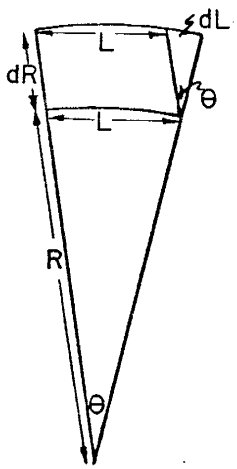

Figure 11, Diagram explaining the fracturing of rock due to regional uplift.

The horizontal expansion is considered to be produced by elastic stretching and a tensile stress T is developed. Under these conditions, a relationship using Young's modulus (E) is valid. Therefore, the relationship $T = E(dL/L)$ exists. From simple geometric relationships where θ is a small angle, it is seen that $L = R\theta$ and $dL = dR\theta$. Consequently, $dL/L = dR/R$. Price (1966) uses an example where 20,000 feet of uplift has occurred (dR). The radius (R) of the earth can be approximated at 4,000 miles. Thus, $dR/R = dL/L$ = approximately 1/1000. Since the rock is under a stress field that causes it to deform in a brittle fashion, this stretch of 1 in 1,000 must be relieved by fracturing (i.e. joint development). Under such circumstances the maximum stress (sigma 1) will be vertical and the intermediate (sigma 2) and minimum (sigma 3) stresses will be perpendicular to each other and in a horizontal plane. Therefore, vertical fractures would form and would be perpendicular to sigma 2 and 3, thus forming an orthogonal pattern.

This is a simplification of the Price model. The patterns developed in nature are not purely orthogonal. Other fracture sets related to the orientation and shape of the basin of deposition are also produced and are not necessarily orthogonal. These are discussed fully by Price (1974) in a later paper.

Models using the propagation of stress fields through "basement" type rocks are presently not favored by many structural geologists (i.e. Price, 1966 and Gibbons, 1981). Surface rocks are thought not capable of transmitting stresses for long distances. For example,

intensely folded areas tend to die out laterally indicating that the stresses are dissipated by strain. Basement rocks are far stronger and more brittle due to confining pressures. It is thought that under these conditions stresses can be laterally transmitted by these rocks. Subsequent transmittal of these stresses vertically through undeformed sedimentary rocks occurs in regions apparently under no lateral stresses forming fractures.

If a basement stress model had a causative effect on the joints in the younger Precambrian sediments, it has to explain the two ages of joint formation. The older fracture set is contained totally within the Apache Group sediments. Evidence that supports this model is the similarity of the older fracture directions (north 5 to 25 degrees east and north 65 to 85 degrees west) in the Apache Group sediments with the older Precambrian structural trends.

Models using earth tides caused by lunar gravitational attractions have been proposed. These forces, however, are substantial but their effect is probably only significant in the uppermost surface of the earth and is not substantial at depth. This model is not favored for the younger Precambrian sediments because it can not explain the two ages of fracturing.

Monoclines

Five monoclines occur throughout the Apache depositional basin. They have a north-south orientation with the east side downdropped. Only one exception exists, in which the west side is down (the Cherry Creek Monocline).

A monocline can be defined as a local sudden steepening in otherwise uniform dipping strata, i.e. a sudden steepening in the dip occurs followed in a short interval by a bend returning the layers to the original structural attitudes.

Rock Canyon Monocline

The Rock Canyon monocline traverses the western edge of the map area. South of the Salt River the monoclinal fold becomes very steep (from the Salt River through Section 23). Apparently, the separation of beds is such in the central and southern portion of Section 23 that a very high angle thrust or normal fault offsets the monocline. This fault diverges to the east of the monocline in the northern portion of Section 23 and dies out; the termination point is hidden by the present location of the Salt River. The maximum offset occurs in the center of Section 23 and is from 100 to 200 feet. As the fault enters the Salt River its displacement is a few tens of feet.

To the north and to the south of Section 23 the monoclinal flexture is less abrupt although the separation of similar beds on each side ranges from 200 to 400 feet (e.g. Fig. 13).

Age and Genesis of Monoclines and Faults

Monoclines can be produced by either compressive or tensional stresses. A monocline is a draping fold generated by plastically deformed sediments overlying a structural offset. The structural offset can be a fault or it can be due to plastically deformed sediments.

EAST approx. 50 ft WEST

Figure 12. Photograph of the Rock Canyon monocline looking south across the Salt River.

WEST EAST

approx. 300 ft.

Figure 13. Photograph of the Rock Canyon monocline looking north across the Salt River (foreground, below picture point).

In a compressive regime the monocline can be envisioned as a thrust (A) or incipient thrust (B) that has died out and is propagated as a draping fold.

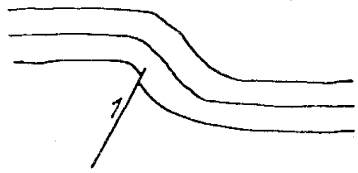

A.

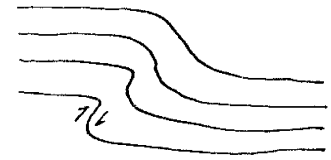

B.

Under a tensional regime the monocline takes the form of a draping fold over a structural offset (fault) (C).

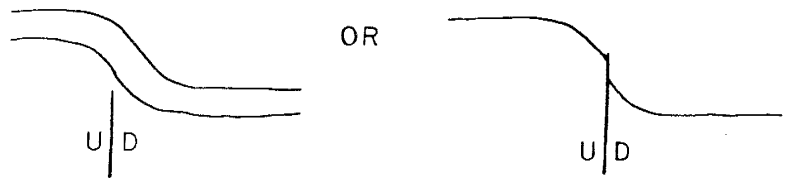

C.

The formative tectonics of a monocline have to be analyzed for each individual monocline. In the case of the monoclines within the younger Precambrian sediments, the causative tectonics are uncertain. Exposures of these monoclines are generally limited to stream drainages that parallel and follow these structures. The Salt River approximately cut the Rock Canyon monocline at a right angle. At this location the underlying tectonics are obscured by large thicknesses of diabase and the relative shallow erosion of the younger Precambrian sediments (limited to the LDSQ, UDSQ and Mescal Limestone).

Underlying the younger Precambrian sediments, the metamorphosed older Precambrian is extensively faulted. Reactivation of these structures in Precambrian times (an idea supported by Shride, 1967) could account for the generation of monoclines. Alternately, the Laramide tectonics that generated monoclines in the Colorado Plateau province could have also generated these monoclines.

The tectonics of monoclines implies the plastic deformation of sediments. In order for this to occur the sediments would have to be unconsolidated or buried to a relatively great depth (at least 10,000 to 15,000 feet). Thicknesses of the younger Precambrian sediments do not change within the monoclinal structures implying that the sediments were well consolidated at the time of folding.

The maximum burial depth of the younger Precambrian sediments is limited during Precambrian times. The total thicknesses of younger Precambrian sediments was estimated by Shride (1967) to be a maximum of 2,650 to 2,800 feet thick. If an equal thickness of diabase is assumed then the maximum burial depth for any portion of younger Precambrian sediments is 5,600 feet or less. The burial of the younger Precambrian during Laramide time was considerably greater than 15,000 feet.

Plastic deformation of the sediments during monocline genesis implies deep burial and, consequently, supports the premise of a Laramide age for the foramtion of these monoclines. This, however, is tentative and speculative and further information is needed to precisely date the monoclines in the younger Precambrian sediments of Gila County, Arizona.

There is only one major fault in the map area. It trends S. 64° E. through Sections 25, 26 and 36, T. 5 N., R. 16 E. and center of Section 31, T. 5 N., R. 17 E. This fault's age is undetermined. It is definitely pre-diabase. The diabase cross-cuts this fault in Section 26, T. 5 N., R. 16 E. (see Plate 1, Geologic map). The evidence does not distinguish whether the fault is pre- or post-monocline.

There is a north-south trending fault in Section 23, T. 5 N., R. 16 E. which seems to be related to the monocline (see Plate 1, Geologic map). It is formed in a very tight portion of the monocline. It appears that this fault pre-dates the diabase sill crossing it. Since the diabase is deeply weathered, this fault possibly could post-date the diabase and is concealed; however, no evidence of a fault in the diabase was seen at this location, thus dating this fault as pre-diabase and Precambrian. This fault is related to the monocline, but it is uncertain whether it acted as a controlling influence on the shape and location of the monocline or was itself generated by the monocline.

GAMMA-RAY SPECTROMETER DATA

Introduction

A reconnaissance geochemical study was done using a Geometric model GR410 gamma-ray spectrometer, analyzing for U, Th and K. The sampling was undertaken concurrently with the measurement of stratigraphic sections in the Snakebit and Regal Canyons, with additional sampling done adjacent to the Tomato Juice uranium mine.

Regionally, the Upper Dripping Spring Quartzite (UDSQ) has been recognized as having a high background radioactivity. In part, this is due to the high potassium content of the rocks, but it is also due to its uranium content.

Theory of Gamma Spectrometry

Radioactive decay produces gamma radiation of many energy levels. The spectrum of gammas produced by an element is characteristic of that element. In gamma spectrometry, a specific energy gamma is counted for each element being analyzed. The quantity of gamma radiation observed is proportional to the concentration of the element.

In this study, a Geometrics model GR410 gamma-ray spectrometer with a model GPX21 detector was used. The Geometrics Corporation has fitted the counting statistics of this instrument to simple linear equations converting field data into chemical analyses (see Table 1).

Errors

The error in gamma-ray spectrometry under field conditions can be expected to be large, because the exact control of the various aspects of gamma-ray spectrometry is not possible. The Geometrics Corporation (1977) has determined the following to be typical errors for the various parameters of this instrument under field conditions:

1) The physical geometry of the sample can cause up to 10% error. The instrument was calibrated for a flat, horizontal surface with the detector one foot above the sample. If sampling is done on the top of a hill, in a small valley, or at a cliff's edge these

TABLE 1

FORMULAS AND CONSTANTS FOR GAMMA-RAY SPECTROMETER ANALYSES

$$\text{Th (ppm)} = (C_{Th} - C_{BG})/\text{sensitivity (Th)}$$

$$\text{U (ppm)} = ((C_U - C_{BG}) - a(C_{Th} - C_{BG})/\text{sensitivity (U)}$$

$$\text{K (\%)} = \frac{((C_K - C_{BG}) - b(C_U - C_{BG}) - g(C_{Th} - C_{BG}))}{\text{sensitivity (K)}}$$

Stripping Constants

$a = 0.62 \pm 0.025$

$b = 0.68 \pm 0.120$

$c = 0.83 \pm 0.170$

Sensitivity Constants

Th = 7.5 ± 0.17 CPM/ppm

U = 20.5 ± 0.87 CPM/ppm

K = 154 ± 50 CPM/T

C_{Th} = counts per minute for Th

C_U = counts per minute for U

C_K = counts per minute for K

C_{BG} = background counts per minute for Th, U and K, repsectively.

errors can be elminated or reduced by multiplying the analysis by the following correction factors suggested by the Geometrics Corporation for ideal geometries: 1.5, 0.75 and 0.666, respectively.

2) Surface moisture content can yield errors of up to 20% in analyses, but these errors are generally less than 10% unless large water contents are encountered.

3) The miscalibration of the instrument can cause a 5% error in analyses.

4) The concentration of an element is calculated using sensitivity and stripping constants. These constants were empirically determined by Geometrics at the Energy Research and Development Administration Test Pads in Grand Junction, Colorado. These constants are designed to correct for Compton scattering developed in the detector crystal and the detector's sensitivity to gamma radiation of various energies. The constants are affected by variations in the source to detector distance. A 5% error is reported for the stripping constants and a 1% error in the sensitivity constant. The author has calculated the worst possible cumulative analytic error due to these constants as 4.5% for Th, 17.9% for U and 44.8% for K.

The calculation of this error was done using the maximum errors for each sensitivity and stripping constants. The maximum and minimum resulting analyses for five samples from the Snakebit Canyon data were used. The errors reported are the average (of the maximum, minus the minimum analyses, divided by 2) for these five samples.

5) Inadequate correction for background radiation is reported to cause an error of 5% at a concentration level of 10 ppm. The background correction is very critical in the 1 ppm range.

6) The counting statistics, i.e. the total number of counts measured, has a 1% error at 10,000 counts. The K measurements made during this study were generally in the range of 10,000 to 15,000 counts, yielding less than 1% error. The U and Th counts ranged from 300 to 2,000 counts causing as much as 6% error in the counting statistics. The % error in counting statistics is calculated by the following relationship: $\%\ \text{error} = \frac{1}{\sqrt{\text{counts}}} \times 100\%$.

The cummulative resulting error can be determined by performing simple calculations using the errors discussed above (see Table 2). The maximum error is expected to be due to the stripping and sensitivity constants, however, counting statistical error was also used to calculate the errors reported in Appendix 1.

The errors due to sample geometry, surface moisture, instrument miscalibration and incorrect background radiation correction were not calculated due to the errors being insignificant or difficult to quantify.

Methodology

During the measurement of stratigraphic sections in Regal Canyon and Snakebit Canyon, gamma-ray spectrometer readings were taken (the data has been plotted on Plate 4). Specific stratigraphic horizons were sampled to characterize them geochemically. At the Tomato Juice mine, additional sampling was done to evaluate any geochemical changes associated with the mineralization.

TABLE 2

Formulas used in Calculating Errors in Gamma-Ray Spectrometer Analyses

$$\text{Maximum Error (Th ppm)} = \pm \frac{(C_{Th} + \frac{C_{Th2}(a)}{6\sqrt{C_{Th2}}} - C_{BG}) - (C_{Th} - C_{BG}/7.5)}{7.5\text{-}0.17(b)}$$

$$\text{Maximum Error (U ppm)} = \pm \frac{(C_U + \frac{C_{U2}(a)}{6\sqrt{C_{U2}}} - C_{BG}) - (0.62\text{-}0.025(c))(C_{Th}-C_{BG})}{20.5\text{-}0.87(b)} - \frac{(C_U + C_{BG}) - 0.62(C_{Th} - C_{BG})}{20.5}$$

$$\text{Maximum Error (K\%)} = \pm \left(C_K + \frac{C_{K2}}{6\sqrt{C_{K2}}} - C_{BG}\right) - (0.68\text{-}0.12(c))(C_U-C_{BG}) - \frac{(0.83\text{-}0.17(c))(C_{Th} - C_{BG})}{154\text{-}50(b)} - \frac{-((C_K-C_{BG}) - 0.68\,(C_U-C_{BG}) - 0.83\,(C_{Th}-C_{BG})}{154}$$

(a) Error due to counting statistics. Note that this error is divided by 6 to convert the data to counts per minute for a six-minute counting interval.
(b) Error due to sensitivity constants.
(c) Error due to stripping constants.

Errors due to the physical geometry of the sample, surface moisture, instrument miscalibration and inadequate background correction were not calculated into the above either because it was thought that the specific analytical error was negligible or it was impossible to quantitatively account for the error.

Constants C_{Th2}, C_{U2} and C_{K2} are total counts.

Constants C_{Th}, C_U, C_K and C_{BG} are in units of counts per minute.

The data was collected by placing the detector directly in contact with the rocks sampled. This caused a change in the stripping and sensitivity constants, causing an unknown error. All samples were collected with the same procedure, thus the absolute analyses may be inaccurate but the data should be relatively consistent.

Counting statistics were gathered by three readings, two minutes in length yielding a total of six-minute counting intervals. In conversations with Phillips Uranium geologists, this counting time was suggested to be the most efficient and yet did not significantly reduce analytic accuracy over longer time periods. The author noted during data collection that three repetitions were vital because it often warned of erratic data when these repetitions did not agree.

Analytical Results

Samples for gamma-ray spectrometry were taken in Regal Canyon at locations previously sampled for chemical analysis. This was done to calibrate the radiometric data with actual chemical analyses. The results of graphic and statistical correlation can be found in Figures 14 and 15. They indicate a linear relationship for equivalent uranium (eU) between 20 and 160 ppm. For values less than 20 ppm, a curvilinear relationship is necessary for the curve to pass through the ordinate. For K, however, the correlation of radiometric with chemical data is uncertain due to the narrow range of values observed and because of the large errors in eK analyses.

COMPARISON OF RADIOMETRIC AND CHEMICAL DATA FOR U IN REGAL CANYON

FIGURE 14

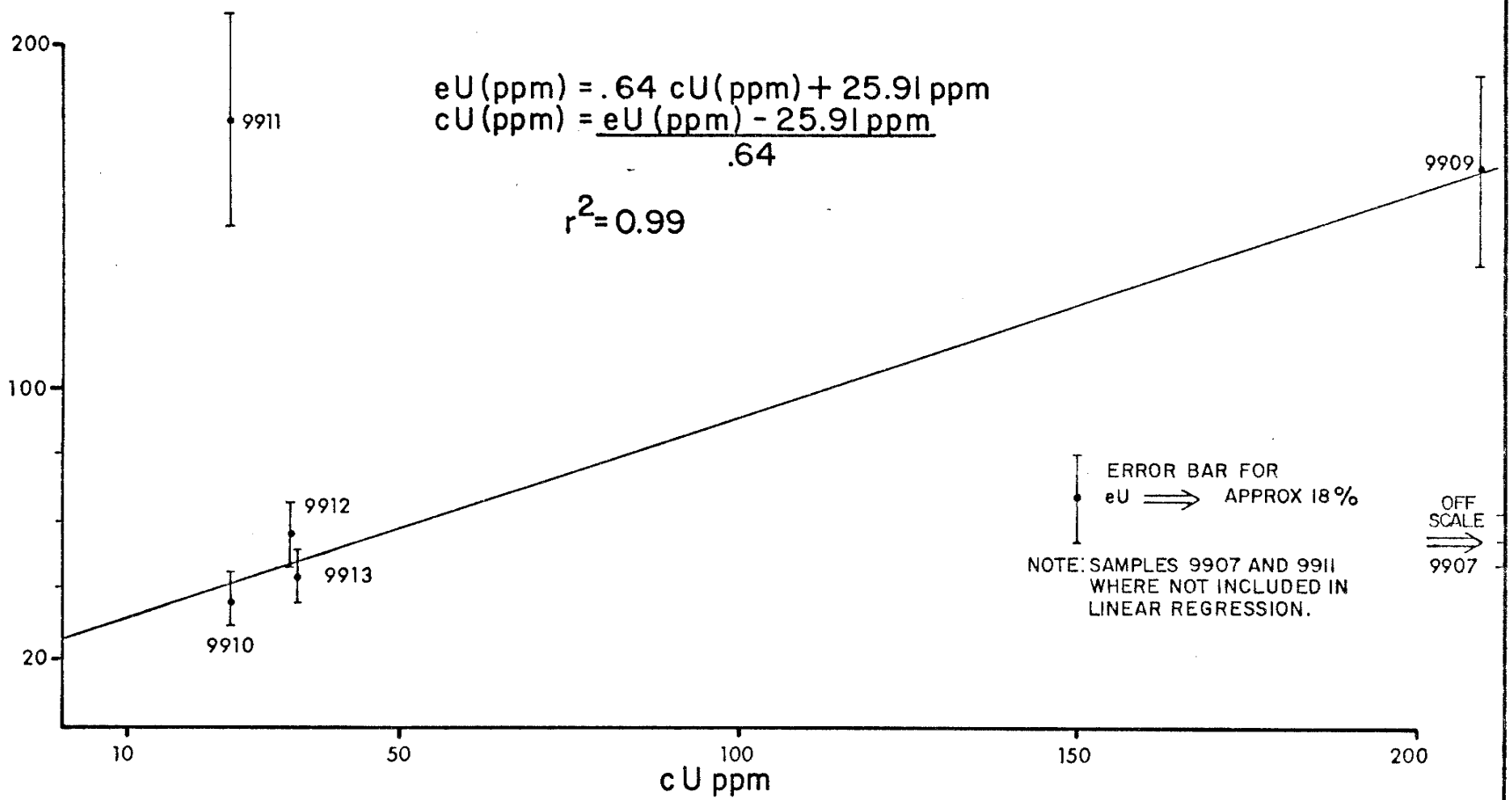

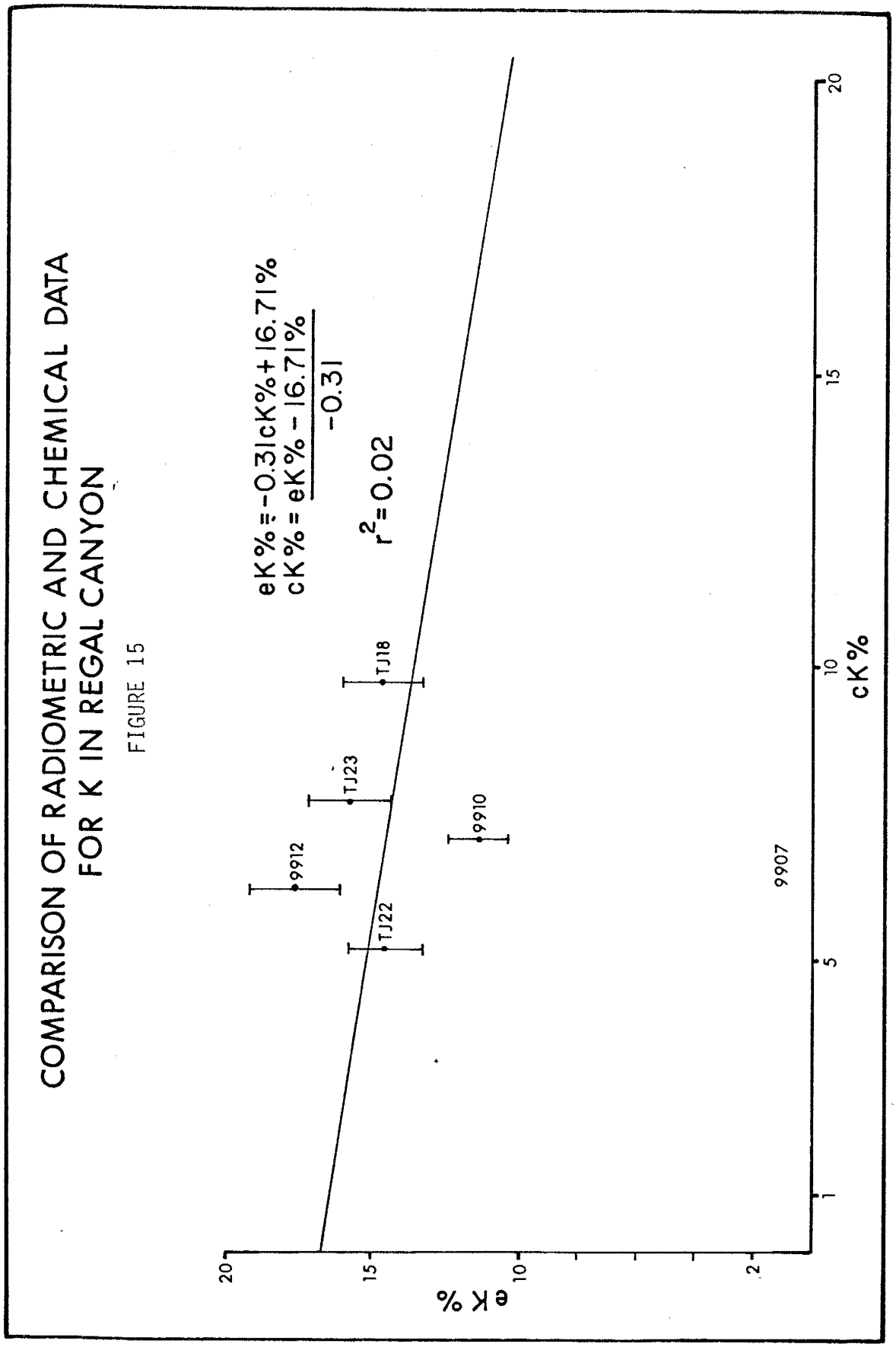
COMPARISON OF RADIOMETRIC AND CHEMICAL DATA
FOR K IN REGAL CANYON
eK% = -0.31cK% + 16.71%
cK% = eK% - 16.71% / -0.31
r² = 0.02
eK%
cK%
9912
TJ22
TJ23
9910
TJ18
9907
20
15
10
2
1
5
10
15
20

FIGURE 15

For this study a correction factor for the sample configuration (as described above) was not applied nor was the data reduced by means of the linear regression discussed above. Quantitative chemical analyses were not carried out as this study was intended to yield semi-quantitative analyses. The data produced should be consistent in a relative sense. A few samples show erroneous analyses, as evidenced in negative K values (see App. I.2, samples 9907, 9909, 9911, GTJ11 and GTJ13).

On Plate 4 the gamma-ray spectrometer data is plotted along side of the measured stratigraphic sections for Regal and Snakebit Canyons. The values of K, U and Th are not precisely correct but it is obvious from the consistency of certain trends in the data that the values are a good approximation of the UDSQ geochemistry. In the Snakebit Canyon data, U and Th data consistently parallel each other. The overall Th/U ratio for the UDSQ is 2.95 with a standard deviation of 0.84 and for the Black facies it is 3.06 with a standard deviation of 0.84. These values are both very close to the accepted average Th/U ratio in igneous rocks of 4.0. This may indicate that the Th and U content in the UDSQ in the Snakebit Canyon represents the ratio of the granitic source rock and little or no in-situ leaching or migration of uranium has occurred.

The K data (see Appendix I.6 and Plate 4) in Snakebit Canyon shows an increase in K in the Black facies and a relative decrease in K in the Black facies and a relative decrease in K in the transitional Black facies zone. This is probably due to a change in the detritus composition which becomes more quartzose in the transition zone.

TABLE 3

WHOLE ROCK ANALYSES

	9903	9905	9907	9910	9912	STJ18	STJ22	STJ23	STJ26
SiO_2	50.4		68.2	63.3	60.7	71.8	64.2	68.2	50.1
TiO_2	0.41		0.68	0.76	0.53	0.24	0.27	0.39	2.06
Al_2O_3	15.0		15.0	15.0	13.9	12.5	14.3	14.0	11.3
Fe_2O_3	19.2	81.51	2.93	6.39	5.82	2.30	3.70	3.30	6.19
MnO	0.21		0.011	0.019	0.13	0.007	0.10	0.044	0.30
MgO	2.14		0.12	0.22	0.26	0.08	0.22	0.06	1.36
CaO	9.35		0.46	0.39	4.31	0.46	4.94	0.80	8.51
Na_2O	4.12		0.34	0.42	0.38	0.59	0.57	0.72	0.62
K_2O	0.88		7.15	8.49	7.46	9.65	6.16	9.22	7.47
P_2O_5	0.12	0.14	9.26	0.10	0.074	0.076	0.12	0.12	0.42
LOI	1.29		2.44	4.85	5.76	1.59	5.22	1.82	11.3
TOTAL	99.42		97.59	99.94	99.32	99.29	99.80	98.65	99.36

Analyses done by Rocky Mountain Geochemical Corporation at their West Jordan, Utah laboratories. Ti and P were analyzed by colorimetry. LOI is the total volitile loss on ignition to 1100°C (includes H_2O+, H_2O^-, CO_2 and others). Fe_2O_3 is calculated from total iron. All other elements were analyzed by atomic absorption. Sample 9903 is diabase, collected at NE¼, SW¼, NE¼, Sec. 36, T. 5 N., R. 17 E. Samples 9907, 9910, 9912, STJ18, STJ22, STJ23 and STJ26 are Black facies and were collected at the Tomato Juice uranium mine (see map, Fig. 16, for location of these samples.

High K values were noted in samples GSB1 and 2 at the base of the Mescal Limestone in the Snakebit Canyon. This could be due to the migration of K from the UDSQ during diagenesis or during the diabase thermal event or it could be due to K metasomatism caused by the intrusion of the diabase. Evidence suggests that there is a diabase feeder zone in Section 31, T. 5 N., R. 17 E. adjacent and to the north of the Snakebit Canyon.

The Regal Canyon geochemistry differs dramatically from the Snakebit Canyon data. The Th/U ratio for the UDSQ in Regal Canyon is 2.13 with a standard deviation of 3.29; and 2.05 for the Black facies with a standard deviation of 4.72, respectively. These numbers are not actually representative, since the data varies significantly (see Table 4). The Black facies actually has a Th/U ratio of 0.4 to 0.5 except for one sample with Th/U=16.90.

Three of the samples in proximity to the Tomato Juice vein show erroneous results; 9907, 9909 and 9911. These results are due to instrument errors probably due to high radiation levels.

The base of the Black facies in Regal Canyon shows a pronounced increase in uranium and a lesser increase in thorium. The data indicates a dramatic drop in K through the lower portion of the Black facies near the Tomato Juice vein, however, this is due to instrument error. Potassium content does not differ significantly when chemical data is analyzed.

TABLE 4

TRACE ELEMENT ANALYSES

	9903	9905	9906	9908	9907	9910	9909	9911	9912	9913
Cu	90	65	235	45	25	25	25	25	70	35
Pb	30	25	430	450	255	50	55	40	30	25
Zn	70	195	315	240	130	20	15	10	15	10
Ni	30	90	100	65	45	35	40	50	50	45
Co	40	35	30	10	5	5	5	-5	5	-5
Cd	-5	5	5	5	5	-5	-5	-5	-5	-5
Mo	1	1	58	495	215	13	32	23	6	4
As	545	15	285	200	105	40	30	35	35	35
Au	-0.1	0.1	-0.1	-0.1	-0.1	-0.1	-0.1	-0.1	-0.1	-0.1
Ag	-1	1	5	5	2	1	1	1	-1	-1
Sb	10	33	10	8	6	2	-1	2	1	2
V_2O_5	-10	130	470	420	320	460	320	460	335	500
Cr	-5	-5	75	70	90	95	80	95	70	80
Be	2	-1	12	13	6	2	2	2	2	2
Se	1	1	4	4	1	-1	4	-1	1	1
W	55	5	5	10	15	10	10	10	5	-5
Bi	-5	-5	-5	-5	-5	-5	-5	-5	-5	-5
Fe%	13.0	54.0	5.73	4.17	2.05	4.47	2.99	4.43	4.07	4.56
F%	0.067	0.009	0.10	0.10	0.047	0.021	0.071	0.021	0.030	0.034
P_2O_5%	0.12	0.14	0.53	0.31	0.26	0.10	0.11	0.10	0.074	0.092
U_3O_8	-1	-1	0.94%	0.51%	0.37%	25	210	25	34	35
C%	-0.1	0.11	-0.1	0.59	-0.01	0.53	0.56	0.53	0.58	0.61
S%	0.19	0.022	4.80	1.12	0.17	0.19	1.88	0.19	0.46	1.80
Ba		0.11%								

Analyses were done by the Rocky Mountain Geochemical Corporation at their Tucson, Arizona laboratories. As, Se, W and P were analyzed by colorimetry, C and S by leco induction furnace, U by fluorometry, F by specific ion electrode and all other by atomic absorption. All values are reported in ppm unless otherwise noted. A negative sign (-) indicates an amount below the minimum detection limit reported).

Data was also plotted as U versus K, Th versus K and U versus Th. The trends observed were different in the Snakebit Canyon than those seen in the Regal Canyon data. The Snakebit Canyon data (see Appendix I.7, I.8 and I.9) exhibits evidence of metasomatic alteration, probably due to the diagenetic alteration of tuffaceous material in the UDSQ, but the time and cause of alteration cannot be determined from the available data. Some of the evidence for the suspected alteration of the Snakebit Canyon area is the high radiometric potassium content observed in the base of the Mescal Limestone (samples GSB1 and 2).

The Regal Canyon gamma-ray spectrometry data, see App. I.3, I.4 and I.5, produced consistent trends: 1) The Upper Dripping Spring Quartzite decreases steadily in K and Th from the base through the top of the formation; 2) Overall, except for the Black facies, the uranium content is relatively constant. The Black facies shows a trend of uranium enrichment at its base and a decrease in the uranium content upwards. The observed uranium trend could be penecontemperaneous with deposition or related to an epigenetic influx or migration of uranium.

The trend in K content can be explained by a decrease in K-rich detritus through time. However, this interpretation is clouded by the anomalous potassium content of the UDSQ, which is most certainly due to tuffaceous, pyroclastic, water-lain material common to the UDSQ.

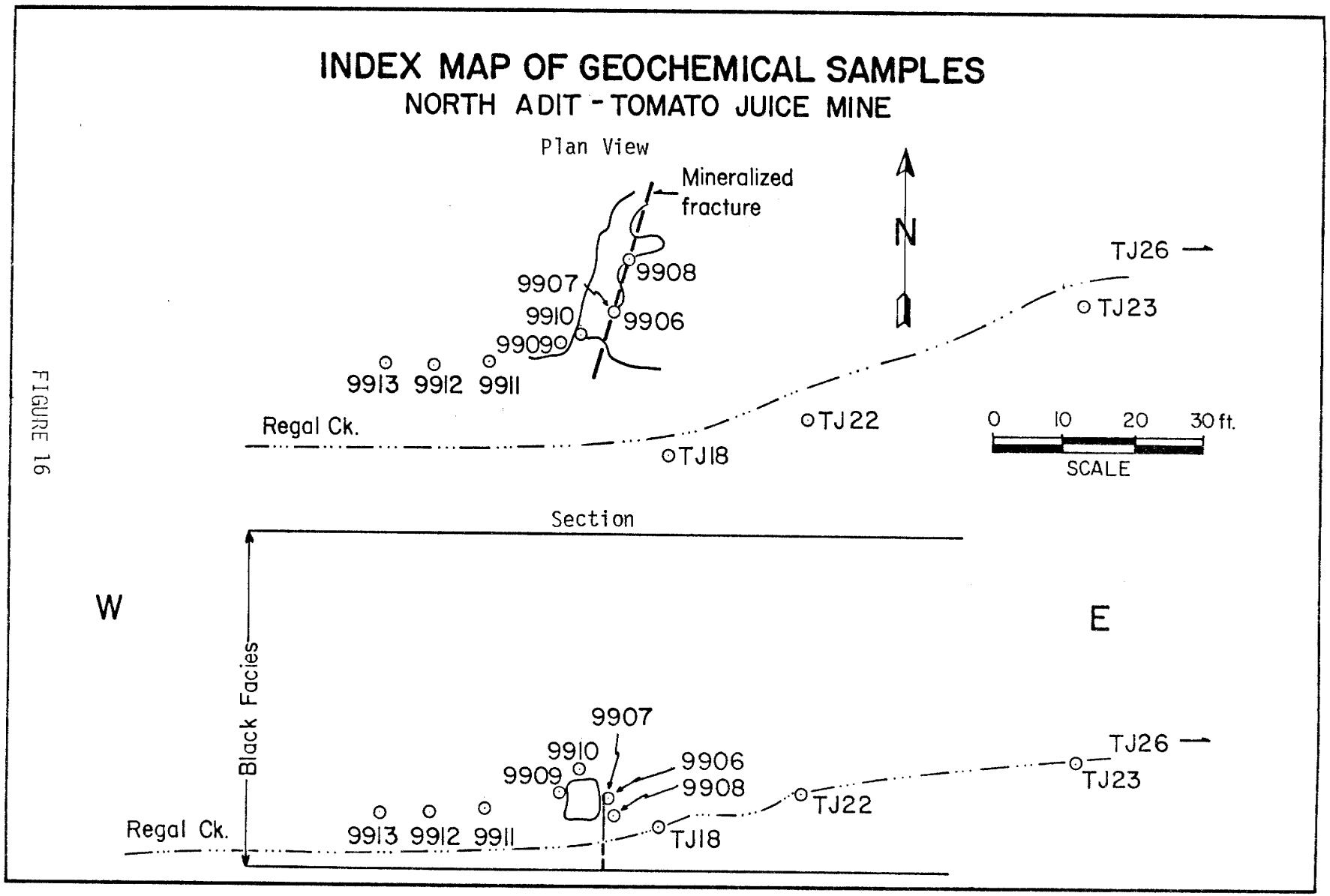
INDEX MAP OF GEOCHEMICAL SAMPLES
NORTH ADIT - TOMATO JUICE MINE
Plan View
Mineralized fracture
N
9907
9908
9910
9906
9909
9913 9912 9911
TJ26
TJ23
TJ22
TJ18
Regal Ck.
0 10 20 30 ft.
SCALE
Section
W
E
Black Facies
9907
9910
9909
9906
9908
9913 9912 9911
TJ26
TJ23
TJ22
TJ18
Regal Ck.

FIGURE 16

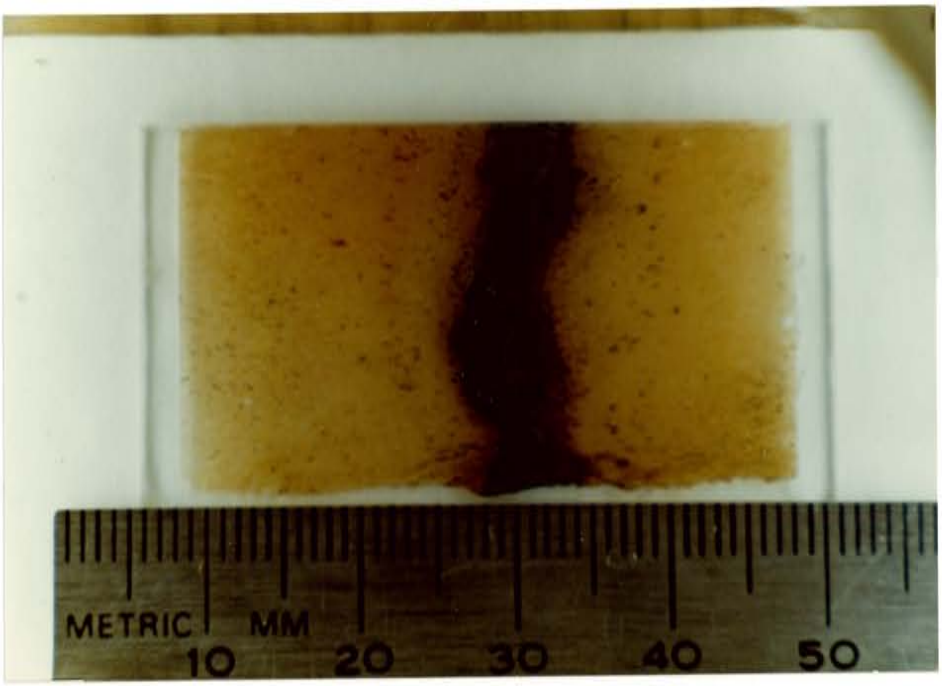

Figure 17. Photograph of polished section (Sample 9906), Tomato Juice vein. Note that the black, very fine sandstone to siltstone host has been "bleached" by the removal of carbon by mineralizing fluids. When compared with Figure 24, it is noted that many of the black spots located in the host "argillite" are an unidentified uranium mineral (probably uraninite). Scale at base of photo is in millimeter divisions.

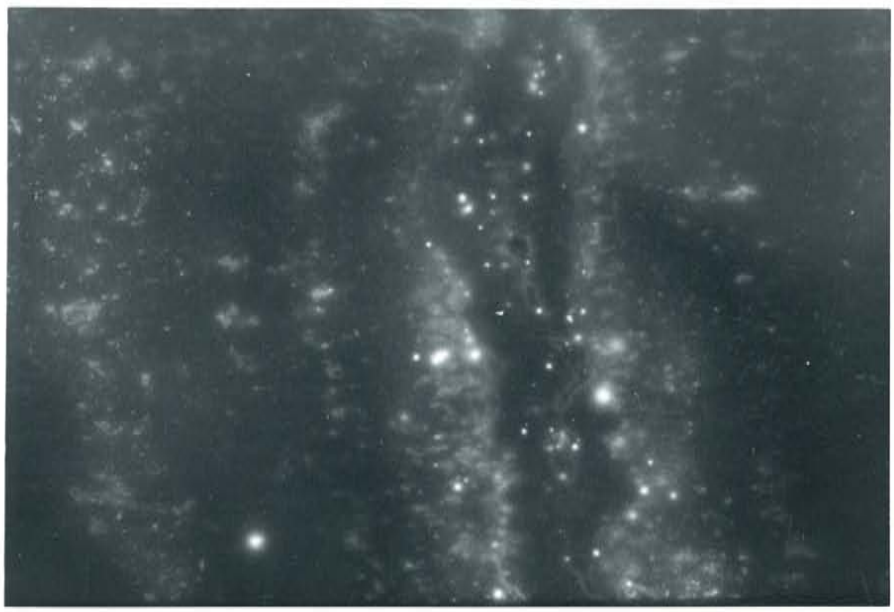

Figure 18. Autoradiograph of polished section (Sample 9906). Shows disseminated uranium mineralization in wall rock, spotted, hot accumulations of uranium in the outer zone of the vein and surrounding the central zone of the vein.

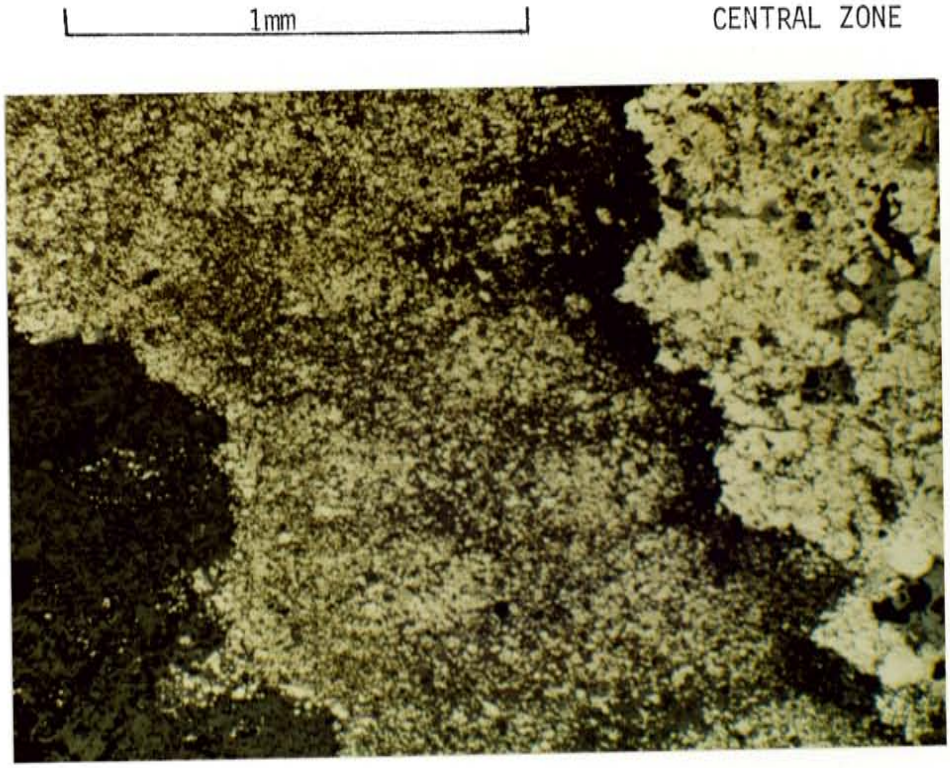

Figure 19. Photograph of polished section (Sample 9906), Tomato Juice vein. Showing two zones within the vein: The outer zone contains pyrite with incomplete replacement of wall rock, the central zone containing pyrite and sphalerite.

0.1 mm

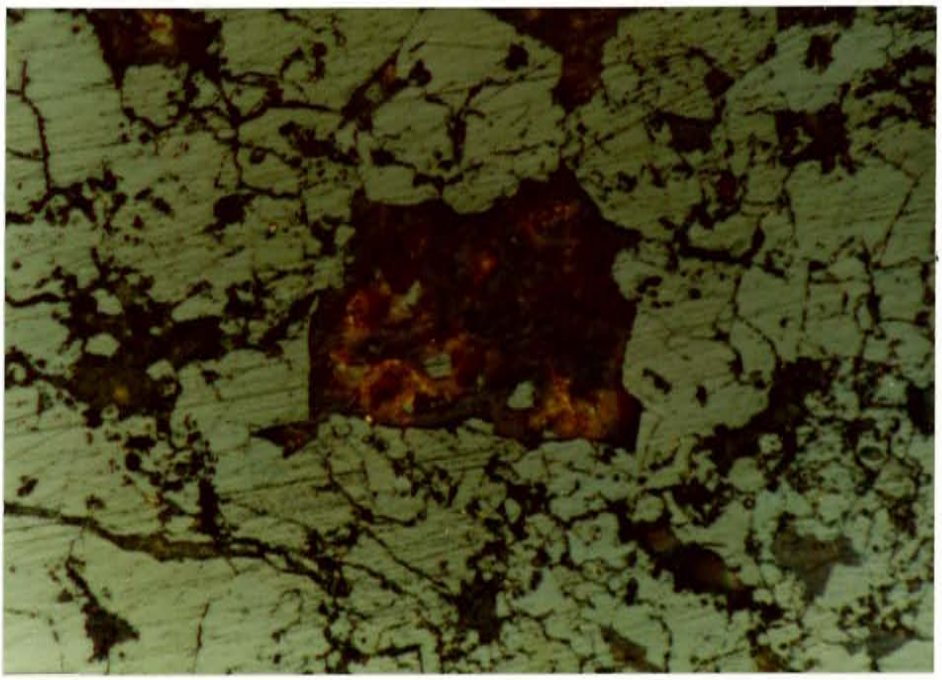

0.1 inch
scale 1:380

Figure 20. Photomicrograph of polished section (Sample 9906). Crossed nicols, showing the textural relationship of sphalerite (center of photo, with honey yellow and reddish internal reflections) with pyrite.

The Th trend can be correlated with a decrease in a resistant detrital trace mineral content. The uranium trend correlates with the trend in uranium vein occurrences. The strict stratigraphic confinement of these veins is curious in that there are similar rock types in the Gray facies and the rest of the Black facies that do not show vein deposits. Also, there does not seem to be any vertical extent to the uranium mineralization outside of the Black facies. In fact, the vein observed at the Tomato Juice mine dies out approximately 15 feet into the Black facies. The lower extent of the vein cannot be observed at this location.

GEOCHEMISTRY

Interpretation of Black Facies Whole Rock Geochemistry

The Black facies of the Upper Dripping Spring Quartzite (UDSQ) has long been recognized to be anomalous in potassium content (Cuffney, 1977; Granger and Raup, 1959, 1964; Williams, 1957 and Smith, 1969), often containing up to 12-14% K_2O. A simple mineralogical model can account for this observed geochemistry.

A mineralogy of potassium feldspar, quartz, muscovite, pyrite ilmenite and calcite in varying quantities is sufficient to explain the observed geochemistry. The potassium enigma is really one of recognizing a mechanism for the origin of the high K-feldspar content of the Black facies. Cuffney (1976) shows evidence (through x-ray data) that the cryptocrystalline layers of a sample consisted almost entirely of microcline, and Granger and Raup (1964) present petrographic evidence that much of the feldspar is authigenic.

Cuffney (1976) notes that very few rocks show chemical analyses of potassium as high as those seen in the UDSQ. He suggests that the K may have been derived from the evaporite beds at the base of the Mescal, which Shride (1967) believed were dissolved and removed during early Mescal times. Thus, diagenesis may well have been largely characterized by the reaction of K-rich fluids with the clay material (probably illite and/or kaolinite) in the UDSQ forming abundant authigenic potassium feldspar. This model, however, does not account for the Na (NaCl, halite) presumably released from the dissolving evaporite beds. It is possible that the Na did not significantly react with the UDSQ and was flushed out of the system by groundwater. The Na content of the Black facies is very low (analyses range from 0.34 to 0.70%). The calcium content is very low also (about 0.5%) and is only high in samples with visible secondary calcite.

Alternately the original sediment, primarily a very fine to silty arkose composed of feldspar, quartz and alteration products of feldspar (clays), could have been authigenically recrystallized during diagenesis. If most of the K-feldspar is of a low temperature origin then much of the Na and Ca would be removed in preference to K. This could explain the low Ca and Na concentrations observed in the Black facies in the Tomato Juice area. Since the Black facies is primarily K-feldspar and quartz, Na and Ca were probably released into and removed by groundwaters. If the present feldspar is a combination of recrystallized detrital feldspar and authigenic feldspar produced by reaction of detrital quartz, clays (probably illite and/or kaolinite) and partially altered detrital feldspars, then the observed whole

rock geochemistry can be explained without the external introduction of K. Therefore, the anomalous K concentration of the Black facies could be due to the reconsitution of the original sediment with a net loss in some elements (Ca, Na, Si and perhaps Mg, which is also in low abundance in the Black facies) with no significant external influence.

It was reported by Heyse (1979) and Lewis Teal (personal communication) that a portion of the Black facies detritus is volcanic in origin. This water transported, tuffaceous material can explain both the whole rock geochemistry and the trace element composition of the Black facies.

The devitrification of volcanic glass and tuffaceous material during diagenesis results in the volcanic material altering to montmorillonitic clays with the release into solution of silica, K, Na, Ca, Mg and trace elements U, V, Ti, Mo, W, Cu, Bi, Zn, Pb, Sb, Hg, Se, Te, As, B, Cl and F (Waters and Granger, 1953). If Na, Ca and Mg are removed from the Black facies in groundwaters then the whole rock major element chemistry is a result of the reaction of K and montmorillonite forming authigenic K-feldspar.

$$2K^{+1} + Al_2Si_4O_{10}(OH)_2 = 2KAlSi_3O_8 + 2HSiO_2$$

montmorillonite K-feldspar

In summary, the Black facies whole rock geochemistry could have a history as follows: First an arkosic sediment (consisting primarily of alkali feldspar and quartz) is deposited with a relatively large quantity of tuffaceous-volcanic detritus (perhaps 10 to 50%). The

volcanic debris is altered during diagenesis forming montmorillonite. During this alteration process K, Na, Ca, Mg and silica are released from the volcanic material. The K and montmorillonite react to form authigenic K-feldspar. The Na, Ca and Mg are preferentially excluded from the low temperature K-feldspar structure and they are subsequently removed by groundwaters. Also, altered and relatively fresh detrital alkali-feldspar could react with the K and silica-rich pore fluid forming additional K-rich feldspar.

Interpretation of the Black Facies Trace Element Geochemistry

A metalliferous black shale model is a possibility for explaining the trace element geochemistry of the Black facies (see Table 6). The general background enrichment of trace metals, especially uranium, could be syngenetic, diagenetic or epigenetic. Since there is a pronounced stratabound nature to the background enrichment of uranium and possibly the trace metals in the Black facies (predominantly confined to the lower 1/4 to 1/3 of the unit), a syngenetic or diagenetic model seems to best explain the Black facies metallogenesis exclusive of the vein deposits.

Vine and Tourtelot (1970) present various processes for the syngenetic enrichment of metals in black shales. Enrichment must occur from the concentration of metals in sea water by living organisms, by decaying organic matter, or by direct sulfide precipitation. Any one of these mechanisms alone cannot account for the amount of metals seen in many black shales when compared with modern processes.

Brongessma-Sanders (1968) suggested a model in which dead planktonic organisms were carried in surface waters long idstances before deposition in black shales. She suggests that this decaying organic matter with its long exposure to fresh sea water would allow anomalously large amounts of trace metals to be absorbed and deposited later in organic-rich shales.

Earlier in this paper a model of stromatolite growth on sandy substrates was presented as a possible model for the Black facies deposition. If this model has credence, then the Brongersma-Sanders model could not apply to the Black facies metallogenesis and would imply that the introduction of trace metals was diagenetic or epigenetic.

Diagenetic enrichment would occur by the influx of externally derived metalliferous fluid prior to complete dewatering of the sediment. This enrichment would further enhance any trace metal anomalies in the original sediment, however, it would be difficult to distinguish it from syngenetic metal enrichments. The source of these metals in a diagenetic model is uncertain. One possible source could be the dissolved evaporite beds, which Shride (1967) postulates to have occurred at the base of the overlying Mescal Limestone, the erosion of the upper Mescal Siltstone and associated basalt flows.

An epigenetic model for the introduction of uranium would have to explain the general stratabound and uniform distribution of trace metals. One recognized major event could offer a mechanism for epigenetic introduction of metalliferous fluids is that of the regional intrusion of diabase sills. Diabase, however, is not generally thought

to be a sufficient source of uranium because of its low uranium content. Another model for the epigenetic introduction of transition metals is the weathering of overlying basalt flows associated with the Mescal. The upper member of the Mescal Limestone was noted to be slightly radioactive in drill holes located in Sections 28 and 29, T. 5 N., R. 17 E. Along with the erosion of basalt flows, this could account for the observed trace elements.

The most plausible model for the formation of the Black facies trace element content is one deriving these metals from detrital, tuffaceous material which is believed to be a significant component in the Black facies sediment. The alteration of the volcanic material during diagenesis would release the following trace elements: U, V, Ti, Mo, W, Cu, Bi, Zn, Pb, Sb, Hg, Se, Te, As, B, Cl and F. The trace element data presented in Table 4 indicates a partial agreement with this suite of trace elements. U, V, Mo, W, Cu, Zn, Pb, Sb, As and F are of normal or anomalous concentration for a carbonaceous, argillitic sediment. W, Bi and Se are low in concentration. Data for Ti, Hg, Te, B and Cl were not obtained for this study. The trace element content of volcanic material can be expected to vary greatly. This could account for the differences between the Black facies and the rocks studied by Waters and Granger (1953). Also, elements released into solution may or may not have been precipitated within the Black facies or carried away by groundwaters.

The Tomato Juice Mine

The Tomato Juice mine was active during the mid- to late-1950's during a period of active uranium interest in the Dripping Spring Quartzite. No production figures are available, but it is apparent that very little ore could have been shipped.

The Tomato Juice mine consists of two short adits that follow a N. 19 to 21° E. trending veinlet. The adits are located along Regal Creek in SE¼, Section 14, T. 5 N., R. 16 E. The north adit is approximately 100 feet long and the south adit 155 feet long. The Tomato Juice vein appears as a hair fracture to a 1/4-inch pinching and swelling pyrite filled vein (see Fig. 23). The vein system is part of the early regional orthogonal fracture system seen throughout the Apache Group sediments in Gila County. The veinlet is extensively cut by a later orthogonal joint system that approximately bisects the early system. The later system shows no evidence of primary mineralization.

The radioactivity is intimately associated with a vertical vein and has apparently spread out horizontally into more permeable horizons forming weakly mineralized manto-like horizons reaching up to several feet from the vein. In other areas of the vein, mineralization falls off rapidly as it enters the wall rock. Within a two- to four-inch wide zone symemetrically on either side of the vein, the gray to black siltstone, argillites and very fine sandstones of the wall rock have been bleached to pink by the removal of carbon by the mineralizing fluids.

Samples 9906 and 9908 were taken on the vein in the north adit of the mine. Sample 9907 is taken four inches west of sample 9906. There are pronounced increases in Pb, Zn, Mo, As, F and U at the vein. There are minor increases at the vein in Cu, Ni, Co, Ag, Sb, Be and P. Fe, Cr and V remain constant through the mineralized zone into the wall rock.

The vein area is enriched with the same metals as the host rock. Thus, it appears that the vein metals are derived from the host rock. That is to say, no external source is necessary to provide a source for these metals.

Granger and Raup (1969) date the vein deposits in the Dripping Spring Quartzite (DSQ) in the Workman Creek area (Sierra Ancha Mountains) at 1060 m.y. This Pb-U isotope concordia-determined age is in agreement with the age of the intrusive diabases associated with the DSQ. It is believed by Heyse (1979) that the ore deposits in the Workman Creek area pre-date the diabase intrusion and that the uranium minerals were recrystallized by this thermal event and the isotopic ages reset. If this is a valid interpretation of the ore textures seen in the Workman Creek (WC) area, and if the vein and stratiform deposits at WC are genetically similar to the Tomato Juice vein, then it can be inferred that the uranium and associated metals were in place prior to the diabase event and this event had little or no effect on the genesis of these veins.

The paragenetic sequence of the Tomato Juice vein from this study seems to be as follows:

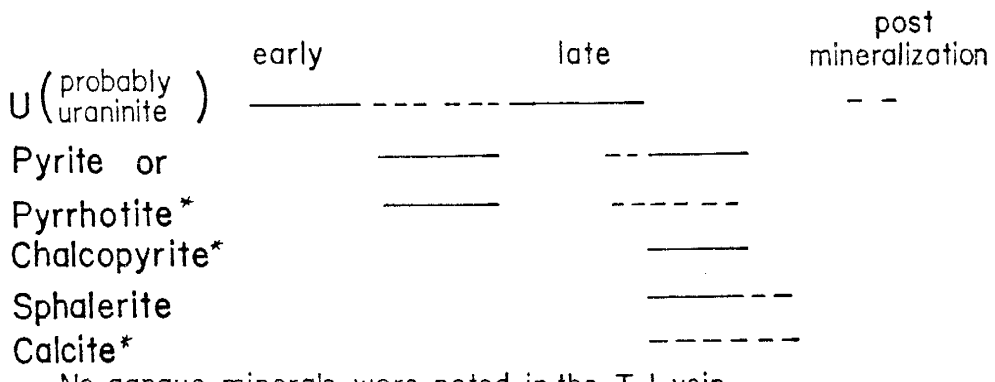

No gangue minerals were noted in the T.J. vein.
* Minerals noted only in sample 9917, from the Walnut Creek prospect; not mentioned in text. sw¼sw¼se¼section 14, T.5N., R.16E.

Granger and Raup (1969) presented a more complete paragenetic sequence for the DSQ veins. It agrees with this study's findings. Early uranium was introduced into the vein system followed by molybdenite, pyrrhotite and pyrite. Then another uranium episode ensued associated with galena and followed by quartz, chalcopyrite, sphalerite and cubanite. Later in the vein history similar minerals were deposited as subsequent redistributions of the vein materials present.

It is believed that the Black facies was enriched in trace metals as a result of the alteration of the volcanic waterlain component of the sediment. These metals were remobilized by groundwater activity caused by an uplift after the deposition of the overlying Mescal Limestone, which also fractured the partially indurated UDSQ. Channeling of these metalliferous fluids within the newly formed fracture system subsequently generated the Tomato Juice vein deposit.

SUMMARY AND CONCLUSIONS

The mineralization of the Upper Dripping Spring Quartzite (UDSQ) has characteristics that suggest the redistribution of anomalous stratiform metal accumulations into a vein system and stratiform deposits. Williams (1957) suggests that the regional, generally orthogonal joint system (north-northeast and west-northwest) that hosts the UDSQ uranium vein deposits is pre-Troy. Joints in these directions are rare in the Troy Quartzite. Since orthogonal joint patterns can form from regional uplifts, the unconformity at the end of Mescal time below the Troy is the most probable time for the development of this early joint system formed in the Apache Group sediments.

This uplift could provide the mechanism for the redistribution of the metals contained within the UDSQ into the recently formed fracture system through groundwater circulation, forming the regionally observed vein uranium deposits. It could also account for the stratiform deposits at Workman Creek, the Lucky Boy mine, the Suckerite mine and the Sky prospect.

Thus, in summary, the formation of uranium deposits (primarily vein deposits) in the UDSQ may have the following sequence (see also Fig. 21): 1) The lower one-third of the Black facies of the UDSQ was deposited with large amounts of volcanic pyroclastic material (perhaps 10-50% of the sediment). Diagenetic alteration of this material released trace metals that remained within the Black facies. During this alteration, abundant K-feldspar was formed and Na, Ca and Mg was removed from the system giving the Black facies anomalous K concentrations.

2) After diagenesis and lithification of the UDSQ, probably at the end of Mescal deposition, a regional uplift occurred. 3) During this uplift a regional orthogonal fracture pattern was developed in the Apache Group sediments forming highly permeable fractures. This uplift also produced hydrodynamic conditions conducive to the strata-bound movement of groundwaters mobilizing U, Fe, Pb, Zn, Cu, Mo, As and F, and to a lesser extent, Ni, Co, Ag, Sb, Be and P. The oxidized zone on either side of the Tomato Juice vein suggests that these metal-bearing solutions may have had a higher eH than the normal connate waters in contact with the Black facies. 4) Permeable zones either fracture-related or stratigraphic-related would preferentially channel these fluids and form the host for the subsequent mineral deposition. 5) Diabase may have overprinted the vein or stratiform deposits by either metamorphic recrystallization as at Workman Creek or by the remobilization of some of the more chemically mobile vein material, but clearly it post-dates the mineralization.

DIAGENESIS OF VOLCANIC GLASS IN THE UPPER DRIPPING SPRING QUARTZITE

GLASS	CLAY	OPAL	MESCAL TIMES ZEOLITE*	LATE OR POST-DIAGENESIS FELDSPAR**
(Henry & Walton, 1978)				
	$Al_2Si_4O_{10}(OH)_2$	SiO_2NH_2O	Na, Ca, Ba, Sr, K Hydrous Aluminosilicate	$(K_n, Na_{1-n})AlSi_3O_8$
	pH rises and Al becomes more soluble but Si remains equally soluble thus forming opal and releasing Al into solution			
U migrates from one phase to another moving distances measured in micrometers or meters and does not form rich U accumulations (the same is probably true of many metals which are probably precipitated as sulfides) (Waters & Granger, 1953)				
	K, Na, Ca, Mg released from the volcanic glass and migrate within the system			K reacts with zeolites or clay to form K felds, Na,Ca, & Mg are removed from the system
	U,V,Ti,Mo,W,Cu,Bi,Zn,Pb,Sb,Hg,Se,Te,As,B,Cl,F are released from the volcanic glass (U,V,Mo,W,Cu,Zn,Pb,Sb,As & F remain within the system)			Mobilized into U-rich deposits

* The opal and zeolite stages of diagenesis are not discussed in text.

** Henry and Walton (1978) do not discuss an authigenic K-feldspar stage.

FIGURE 21

REFERENCES CITED

Anderson, C. A., 1951, Older Precambrian structure in Arizona: GSA Bull., Vol. 62, p. 1331-1346.

Brongersma-Sanders, M., 1968, On the geographical association of strata-bound ore deposits with evaporites: Mineralia Deposita, Vol. 3, p. 286-291.

Cuffney, R. G., 1976, Geology of the White Ledges area, Gila County, Arizona: Unpublished M.S. Thesis, Colorado School of Mines, Golden, Colorado.

Deer, W. A., Howie, R. A. and Zussman, J., 1966, An introduction to the rock-forming minerals: Longman Group Limited, London, 528 p.

Gastil, R. G., 1953, Geology of the eastern half of the Diamond Butte quadrangle, Gila County, Arizona: Unpublished Doctoral Dissertation, University of California, Berkeley, California.

Geometrics Corporation, 1977, Technical manual for portable gamma-ray spectrometer model GR-410 with detector models GPX-21, GPX-6 or GPX-110, Vol. 1, Operation: Geometric Inc./Exploration Corporation Canada, Ltd., Toronto, Canada.

Gibbons, J., 1981, Lecture given at the University of New Mexico on the origin of regional fracture patterns, February 19, 1981.

Glossary of Geology, 1977, Gary, M., McAfee, R., Jr. and Wolf, C. L., editors: American Geological Institute, Washington D.C.

Granger, H. C. and Raup, R. B., Jr., 1959, Uranium deposits in the Dripping Spring Quartzite, Gila County, Arizona: U.S.G.S. Bull. 1046-P, p. 415-486.

Granger, H. C. and Raup, R. B., Jr., 1964, Stratigraphy of the Dripping Spring Quartzite, southeastern Airzona: U.S.G.S. Bull. 1168, 119 p., illus. and tables.

Henry, C. D. and Walton, A. W., 1978, Formation of uranium ores by diagenesis of volcanic sediments: U.S. Dept. of Energy, GJBX 22-79.

Heyse, J. V., 1979, The mineralogy and paragenesis of the Dripping Spring uranium deposits, Gila County, Arizona, with emphasis on the Workman Creek area: Unpublished company report, Wyoming Minerals Corporation.

Kelley, V. C., 1955, Regional tectonics of the Colorado Plateau and relationship to the origin and distribution of uranium: University of New Mexico Publications in Geology, Number 5, The University of New Mexico Pre-s, 120 p.

Kelley, V. C. and Clinton, N. J., 1960, Fracture systems and tectonic elements of the Colorado Plateau: University of New Mexico Publications in Geology, Number 6, The University of New Mexico Press.

Kessler, G., 1981, Stratigraphy of the Upper Dripping Spring Quartzite: Unpublished in-house report, Phillips Uranium Corporation.

Livingston, D. E., 1969, Geochronology of older Precambrian rocks in Gila County, Arizona: Unpublished Doctoral Dissertation, University of Arizona, Tucson, Arizona.

Neurburg, G. J. and Granger H. C., 1960, A geochemical test of diabase as an ore source for the uranium deposits of the Dripping Spring district, Arizona: Neuves Jahrbuch fur Mineralogie, Bd. 94, p. 759-797, illus., Stuttgart, Germany.

Park, R. K., Kessler, G. and Teal, L., 1981: Unpublished in-house report, Phillips Uranium Corporation.

Price, N. J., 1966, Fault and joint development in brittle and semi-brittle rock: Pergamon Press Ltd., 176 p.

Price, N. J., 1974, The development of stress systems and fracture patterns in undeformed sediments: in the 3rd International Soc. Rock Mechanics Proc., Vol. 1, p. 487-496.

Ransome, F. L., 1903, Geology of the Globe copper district, Arizona: U.S.G.S. Prof. Paper 12, 168 p.

Showalter, S., 1980, Personal communication.

Shride, A. F., 1967, Younger Precambrian geology in southern Arizona: U.S.G.S. Prof. Paper 566, 89 p.

Silver, L. T., 1960, Age determinations on Precambrian diabase differentiates in the Sierra Ancha, Gila County, Arizona(abs.): GSA Bull., Vol. 71, p. 1973-1974.

Smith, D., 1969, Mineralogy and petrology of an olivine diabase sill complex and associated unusually potassic granophyres, Sierra Ancha, central Arizona: Unpublished Doctoral Dissertation, California Institute of Technology, Pasadena, California, 1969.

Vine, J. D. and Tourtelot, E. B., 1969, Geochemistry of black shale deposits - A summary report: Economic Geology, Vol. 65, p. 253-272.

Waters, A. C. and Granger, H. C., 1953, Volcanic debris in uraniferous sandstones and its possible bearing on the origin and precipitation of uranium: U.S.G.S. Circ. 224.

Williams, F. J., 1957, Structural control of uranium deposits, Sierra Ancha region, Gila County, Arizona: U.S.A.E.C. RME-3152, 121 p.

Wilson, E. D., 1939, Precambrian Mazatzal revolution in central Arizona: GSA Bull., Vol. 50, p. 1113-1163.

APPENDIX I

GAMMA-RAY SPECTROMETER DATA

GAMMA-RAY SPECTROMETER CALIBRATION DATA
(Readings in counts per minute)

H.B. Calibration point (concrete patio)

K	452.00	452.33	438.67	469.50	511.00	501.50	481.50	491.67	492.33	501.33	556.83	K
U	92.50	95.17	92.50	93.17	97.00	97.33	89.17	90.00	98.00	93.00	97.67	U
Th	77.00	74.33	79.00	82.83	73.67	77.83	77.33	73.83	77.50	74.00	67.17	Th

TJCPT 1 (Mescal L.S. calibration point)

K	46.17	69.33	K
U	44.33	46.67	U
Th	18.55	20.67	Th

TJCPT 2 (Background: read over water)

K	102.50	96.17	100.67	108.50	99.17	115.17	109.33	K
U	49.83	38.67	36.50	45.83	36.83	45.83	43.17	U
Th	18.83	20.00	19.17	25.17	21.67	17.50	23.33	Th

Note: The values given in this table were generated to evaluate instrument drift. No significant drift was observed. The data is the average of three, two-minute counting intervals (six minutes total).

DATE	9/09/80	9/10/80	10/09/80	10/11/80	10/13/80	10/14/80	10/15/80	10/21/80	10/23/80	10/26/80	10/27/80	10/28/80	12/04/80	DATE

GAMMA-RAY SPECTROMETER DATA

REGAL CANYON - TOMATO JUICE MINE

	eK	±	eU	±	eTh	±	Th/U
G9907	-19.61	-----	49.16	8.80	515.18	20.45	10.48
G9909	-15.59	-----	160.43	28.72	24.13	2.49	0.15
G9910	10.66	4.78	36.96	6.62	20.29	2.26	0.55
G9911	-11.78	-----	177.35	31.75	15.04	1.92	0.08
G9912	17.61	7.89	57.66	10.32	14.44	1.88	0.25
G9913	16.60	7.44	43.65	7.81	12.87	1.77	0.29
GTJ28	0.43	0.19	2.06	0.37	0.44	0.62	0.21
GTJ27	6.77	3.03	1.16	0.21	4.47	1.06	3.85
GTJ26	9.14	4.09	3.88	0.69	4.73	1.09	1.22
GTJ25	10.36	4.64	2.14	0.38	9.20	1.47	4.30
GTJ24	10.59	4.74	19.15	3.43	16.04	1.96	0.84
GTJ23	14.00	6.27	4.23	0.76	10.82	1.59	2.56
GTJ22	12.15	5.44	5.15	0.92	10.49	1.57	2.04
GTJ21	13.68	6.13	7.50	1.34	11.40	1.64	1.52
GTJ20	14.63	6.55	7.20	1.29	10.60	1.58	1.47
GTJ19	15.75	7.06	18.17	3.25	12.98	1.75	0.71
GTJ18	14.44	6.47	29.83	5.34	14.60	1.86	0.49
GTJ17	15.11	6.77	44.66	7.99	14.98	1.89	0.34
GTJ16	11.66	5.22	46.10	8.25	17.33	2.05	0.38
GTJ15	14.49	6.49	65.33	11.69	17.89	2.08	0.27
GTJ14	16.29	7.30	87.58	15.68	18.18	2.10	0.21
GTJ13	-12.32	-----	143.24	25.64	19.53	2.19	0.14
GTJ12	3.54	1.59	9.60	1.72	162.22	8.54	16.90
GTJ11	-13.31	-----	147.62	26.42	15.09	1.90	0.10
GTJ10	14.89	6.67	30.20	5.41	17.53	2.09	0.58
GTJ9	14.78	6.62	16.53	2.96	14.93	1.91	0.90
GTJ8	9.37	4.20	7.96	1.42	13.91	1.84	1.75
GTJ7	14.05	6.29	6.55	1.17	15.49	1.95	2.36
GTJ6	14.54	6.51	11.07	1.98	16.09	1.99	1.45
GTJ5	14.77	6.62	5.33	0.95	17.47	2.08	3.28
GTJ4	15.01	6.72	6.68	1.20	20.20	2.26	3.02
GTJ3	15.42	6.91	7.42	1.33	18.15	2.13	2.45
GTJ2	18.28	8.19	7.62	1.36	23.69	2.47	3.11
GTJ1	14.17	6.35	4.73	0.85	18.91	2.17	4.00
	%	±	ppm	±	ppm	±	

Negative (-) K values are probably produced by large errors in counting statistics due to Compton scattering in high uranium samples. Errors in analyses are uncertain but are expected to be less than 4.5% for Th, 17.9% for U and 44.8% for K (see text for further explanation). See Plate 4 for the general stratigraphic location of these samples.

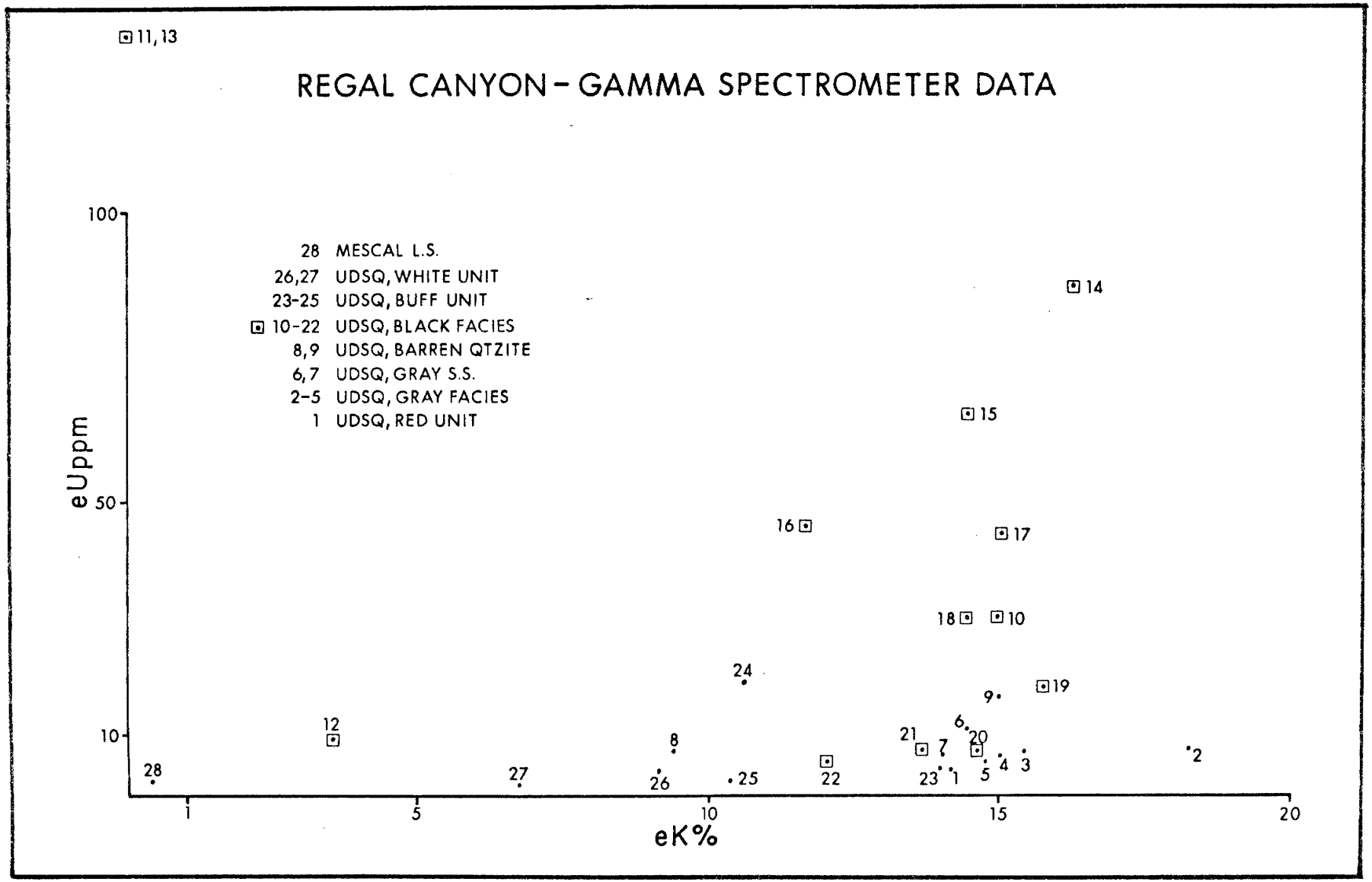
REGAL CANYON - GAMMA SPECTROMETER DATA
28 MESCAL L.S.
26,27 UDSQ, WHITE UNIT
23-25 UDSQ, BUFF UNIT
10-22 UDSQ, BLACK FACIES
8,9 UDSQ, BARREN QTZITE
6,7 UDSQ, GRAY S.S.
2-5 UDSQ, GRAY FACIES
1 UDSQ, RED UNIT
eUppm
100
50
10
eK%
1
5
10
15
20
11, 13
14
15
16
17
18
10
19
24
9
12
8
6
21
7
20
28
27
26
25
22
23
1
5
4
3
2

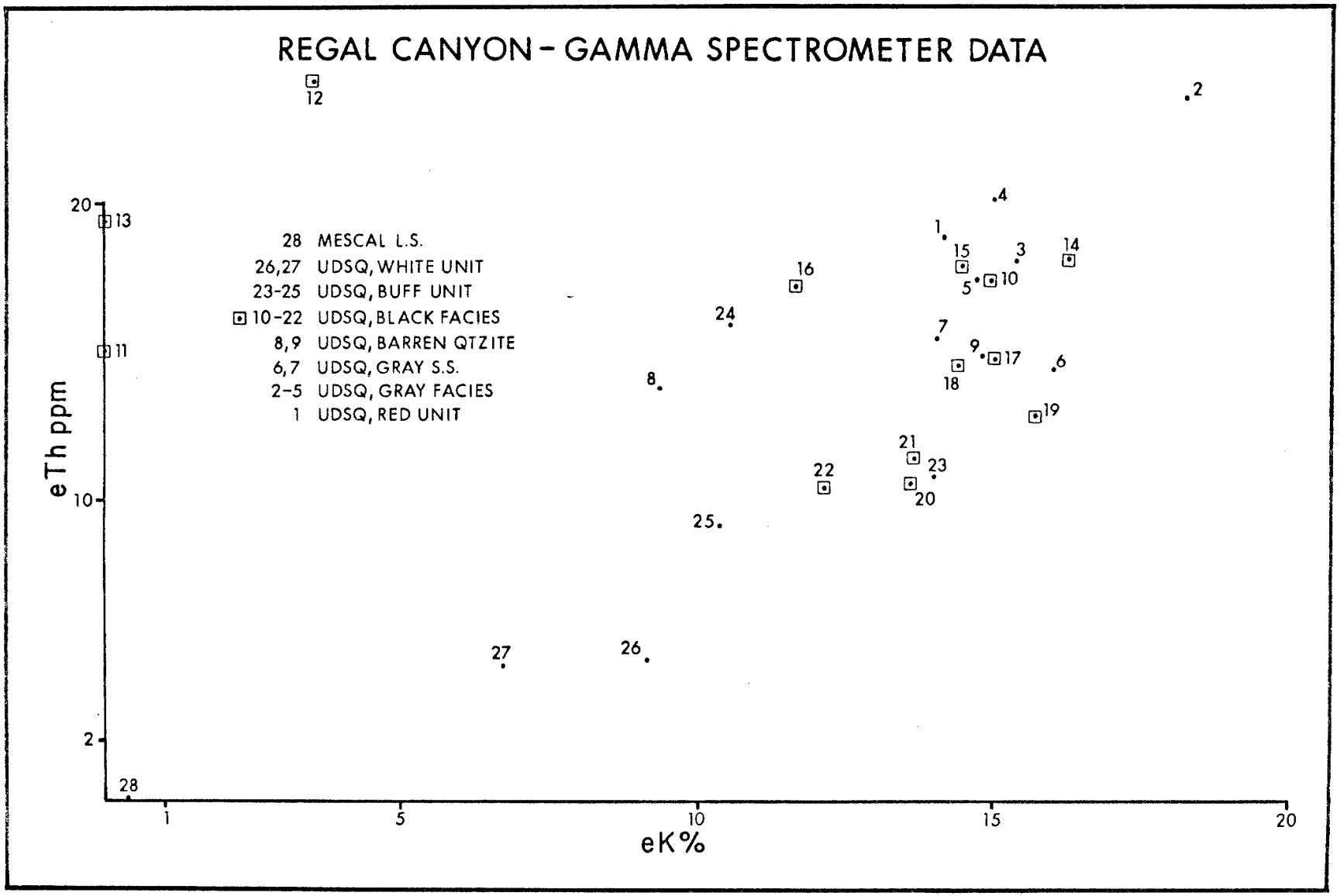
REGAL CANYON - GAMMA SPECTROMETER DATA
28 MESCAL L.S.
26,27 UDSQ, WHITE UNIT
23-25 UDSQ, BUFF UNIT
10-22 UDSQ, BLACK FACIES
8,9 UDSQ, BARREN QTZITE
6,7 UDSQ, GRAY S.S.
2-5 UDSQ, GRAY FACIES
1 UDSQ, RED UNIT
eTh ppm
eK%
20
11
10
2
1
5
10
15
20

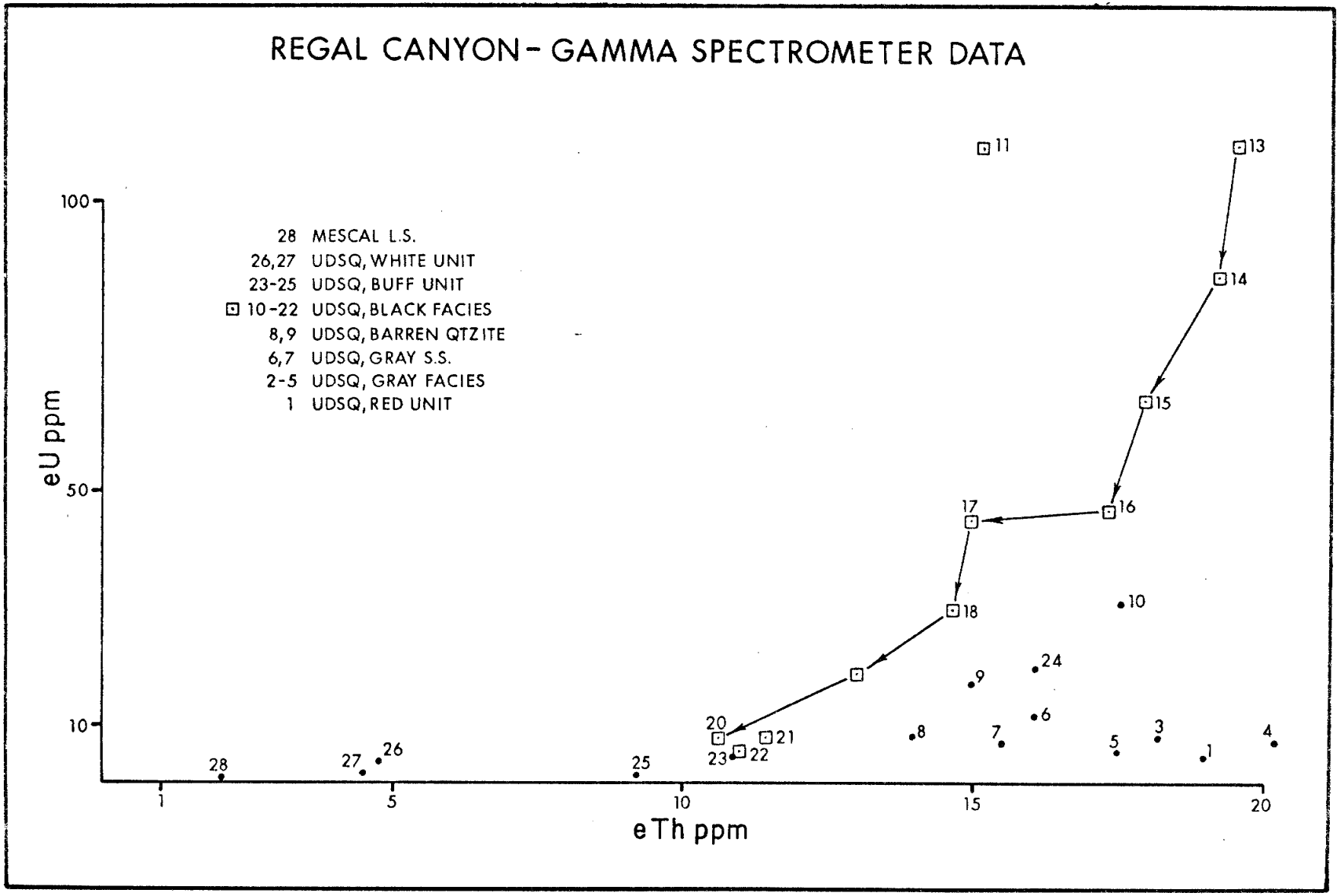
REGAL CANYON - GAMMA SPECTROMETER DATA
28 MESCAL L.S.
26,27 UDSQ, WHITE UNIT
23-25 UDSQ, BUFF UNIT
10-22 UDSQ, BLACK FACIES
8,9 UDSQ, BARREN QTZITE
6,7 UDSQ, GRAY S.S.
2-5 UDSQ, GRAY FACIES
1 UDSQ, RED UNIT
eU ppm
100
50
10
eTh ppm
1
5
10
15
20

GAMMA-RAY SPECTROMETER DATA
SNAKEBIT CANYON

	eK	±	eU	±	eTh	±	Th/U
GSB1	6.89	3.09	1.18	0.21	0.51	0.67	0.43
GSB2	7.38	3.31	0.94	0.17	2.49	0.90	2.65
GSB3	7.73	3.46	0.91	0.16	3.27	0.98	3.59
GSB4	13.40	6.00	2.95	0.53	8.15	1.41	2.76
GSB5	14.37	6.44	2.92	0.52	11.47	1.67	3.93
GSB6	10.63	4.76	2.49	0.45	10.51	1.59	4.22
GSB7	11.83	5.30	2.43	0.43	10.02	1.56	4.12
GSB8	15.35	6.88	3.85	0.69	12.80	1.76	3.32
GSB9	18.71	8.38	7.57	1.36	12.07	1.71	1.59
GSB10	19.11	8.56	6.01	1.08	13.13	1.78	2.18
GSB11	17.41	7.88	4.16	0.74	13.13	1.71	3.16
GSB12	17.85	8.00	4.55	0.81	12.55	1.74	2.76
GSB13	18.73	8.39	4.06	0.73	13.33	1.80	3.28
GSB14	17.20	7.71	4.15	0.74	11.95	1.70	2.88
GSB15	15.65	7.01	10.43	1.87	18.87	2.17	1.81
GSB16	12.96	5.81	6.31	1.13	11.04	1.63	1.75
GSB17	6.24	2.80	3.88	0.69	11.44	1.66	2.95
	%	±	ppm	±	ppm	±	

Errors in analyses are uncertain but are expected to be less than 4.5% for Th, 17.9% for U and 44.8% for K (see text for explanation). See Plate 4 for the general stratigraphic location of these samples.

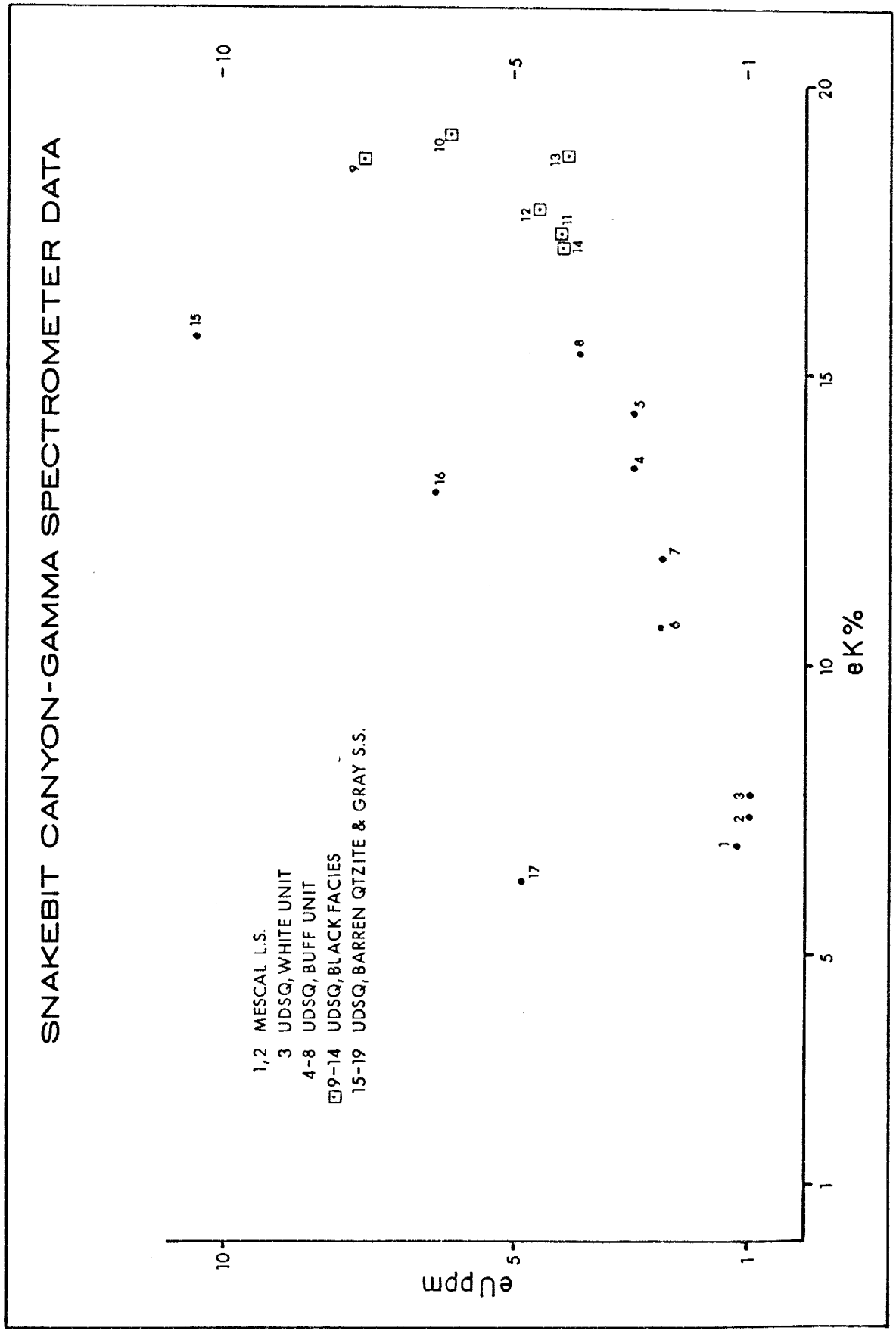
SNAKEBIT CANYON-GAMMA SPECTROMETER DATA
1,2 MESCAL L.S.
3 UDSQ, WHITE UNIT
4-8 UDSQ, BUFF UNIT
9-14 UDSQ, BLACK FACIES
15-19 UDSQ, BARREN QTZITE & GRAY S.S.
eU ppm
eK %
10
5
1
1
5
10
15
20
-10
-5
-1

SNAKEBIT CANYON - GAMMA SPECTROMETER DATA

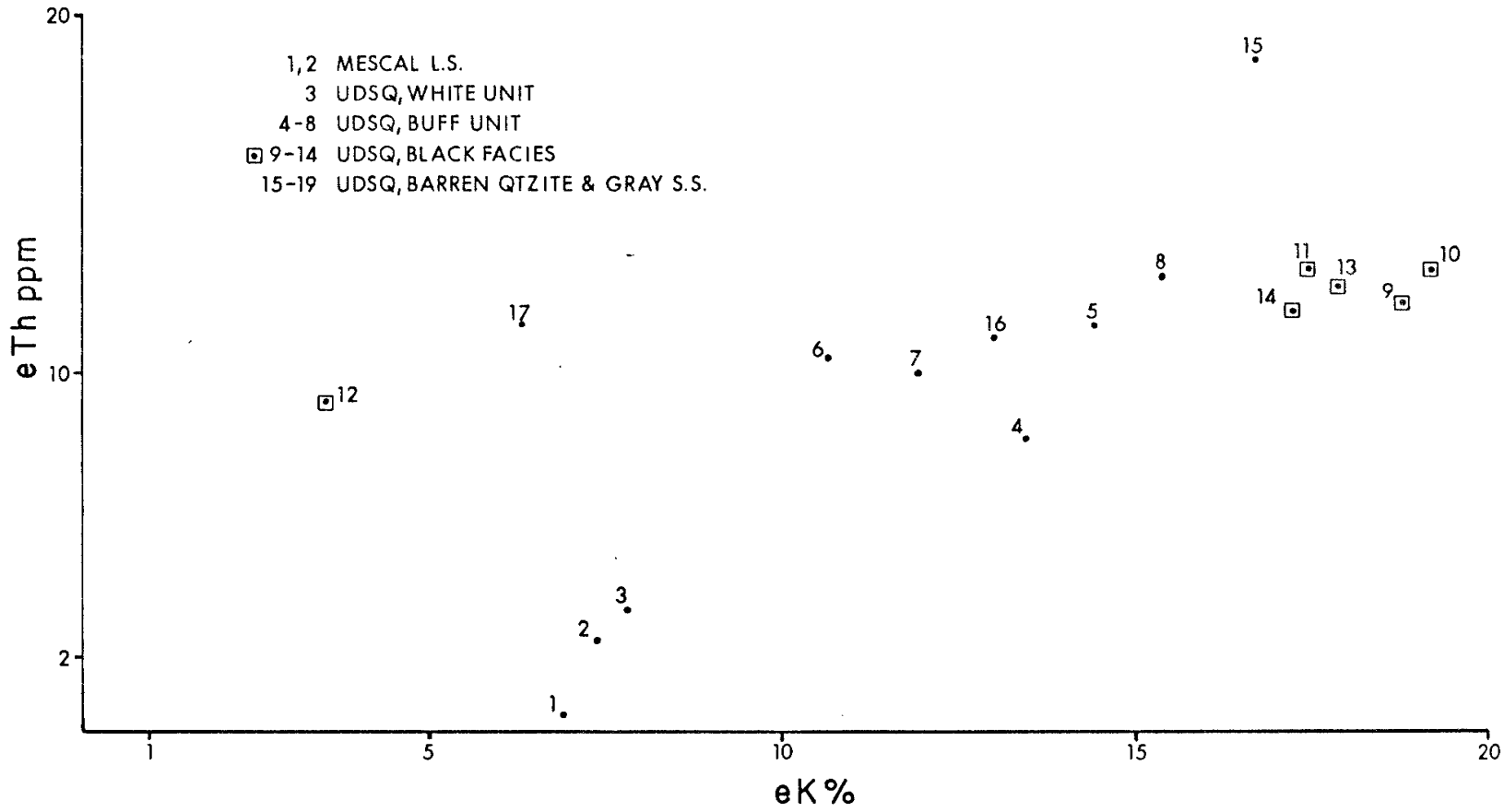

SNAKEBIT CANYON - GAMMA SPECTROMETER DATA

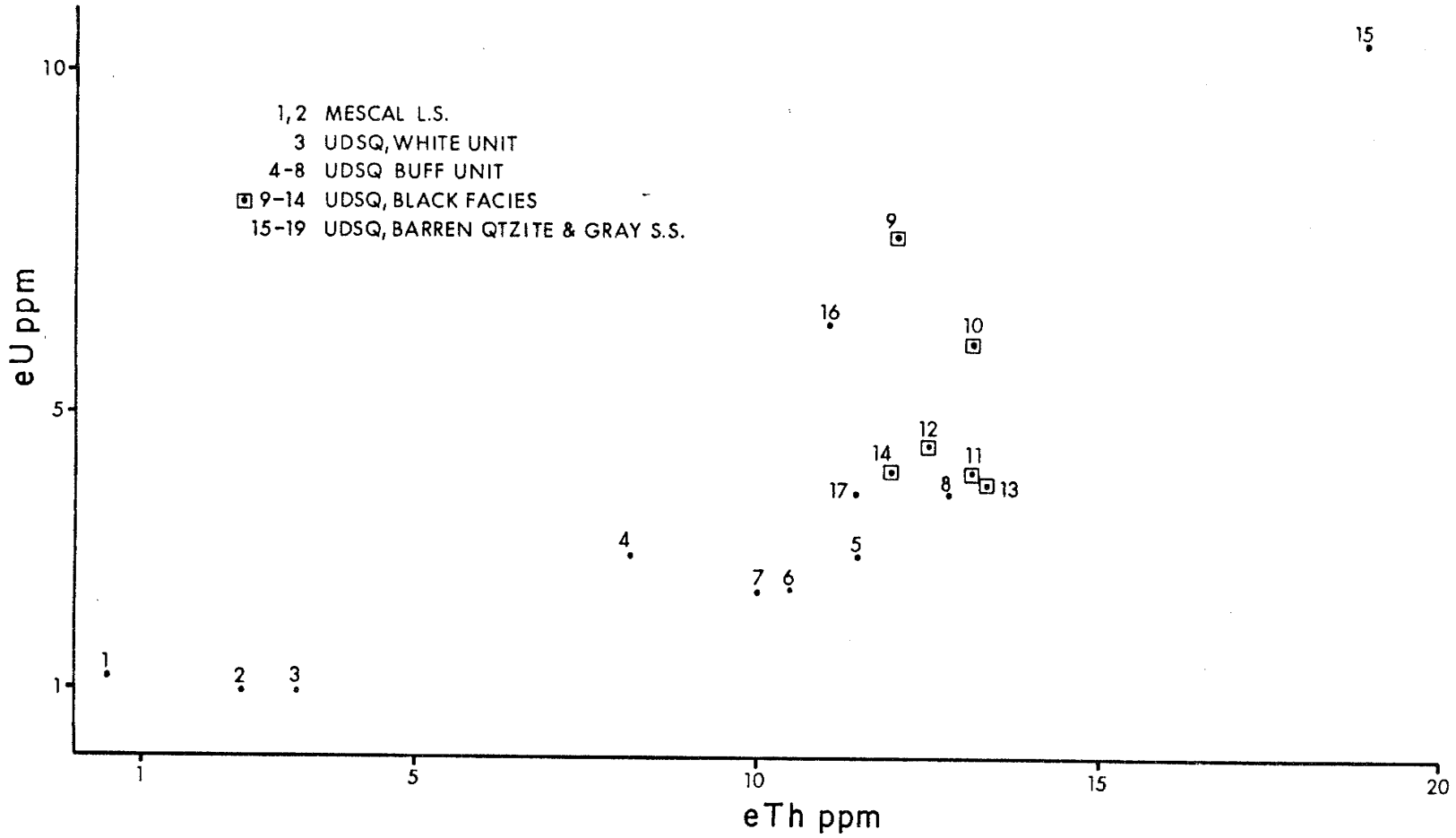

This thesis is accepted on behalf of the faculty of the Institute by the following committee:

Clay T. Smith
Adviser

9/28/81
Date